

ENGINEERING BETTER PROTECTIVE HEADGEAR  
FOR  
SPORT AND MILITARY APPLICATIONS

A Thesis

Submitted to the Faculty

of

Purdue University

by

Kevin G. McIver

In Partial Fulfillment of the

Requirements for the Degree

of

Master of Science in Mechanical Engineering

May 2019

Purdue University

West Lafayette, Indiana

**THE PURDUE UNIVERSITY GRADUATE SCHOOL**  
**STATEMENT OF THESIS APPROVAL**

Dr. Eric A. Nauman, Chair

School of Mechanical Engineering and  
Weldon School of Biomedical Engineering

Dr. Thomas M. Talavage

School of Electrical and Computer Engineering and  
Weldon School of Biomedical Engineering

Dr. Jan-Anders Mansson

School of Materials Engineering and Chemical Engineering

**Approved by:**

Dr. Jay Gore

Associate Head for Graduate Studies, Mechanical Engineering

To my parents, David and Ann McIver without whom none of this would be possible.

## ACKNOWLEDGMENTS

I'd like to extend thanks to those who have helped me along the way, both through three years of undergraduate research and graduate work. I'd like to begin by thanking Dr. Eric Nauman and Dr. Thomas Talavage, who've guided me through my undergraduate research and graduate research. I thank Dr. Nauman for providing the advice and teaching me all aspects of being a good engineer. I thank Dr. Talavage for his assistance in making sure I present data with meaning with strong statistical groundings.

I also thank Dr. Jan-Anders Mansson for agreeing to be on my committee and the Composite Manufacturing and Simulation Center's advice (in particular that of Dr. Josh Dustin) on improving manufacturing techniques for our composite helmets.

I'd like to thank each of the graduate and undergraduate students in the HIRRT Lab for the last 4 years, in particular, Roy Lycke, Taylor Lee, Michael Dziekan, Nicolas Leiva, and Goutham Sankaran. Thanks also to undergraduates Sean Bucherl and Patrick Lee for collecting data in some of the impact testing.

I would also like to take the time to thank my brother, and my grandparents: you have all been a great source of life advice, and I love and appreciate you more than you know.

I would also like to thank the Alfred P. Sloan foundation through the Sloan Indigenous Graduate Partnership, the Cordier family, and the Chickasaw Nation Higher Education Foundation who provided support for my work in the form of graduate fellowships and scholarships.

## PREFACE

The basis for this research stemmed from my interest in developing better technology to prevent long term damage to football players and servicemen. As this technology matures hopefully it can be incorporated into protective equipment for military applications. Now, in the words of Dr. Nauman, we're going to "engineer the s\*\*t" out of helmets.

## TABLE OF CONTENTS

	Page
LIST OF TABLES . . . . .	viii
LIST OF FIGURES . . . . .	xi
ABBREVIATIONS . . . . .	xiv
ABSTRACT . . . . .	xv
1. INTRODUCTION . . . . .	1
2. BACKGROUND . . . . .	3
2.1 Current Methodologies . . . . .	3
2.2 A Non-Dimensional Framework to Assess the Performance of Helmets in Sport and Military Applications . . . . .	7
2.2.1 Theory . . . . .	8
2.2.2 Data Collection . . . . .	10
2.2.3 Statistical Analysis . . . . .	14
3. SOCCER HEADGEAR . . . . .	17
3.1 Abstract . . . . .	17
3.2 Introduction . . . . .	17
3.3 Methods . . . . .	18
3.4 Results . . . . .	19
3.5 Discussion . . . . .	24
4. LACROSSE HELMETS . . . . .	27
4.1 Abstract . . . . .	27
4.2 Introduction . . . . .	27
4.3 Methods . . . . .	28
4.4 Results . . . . .	29
4.5 Discussion . . . . .	35
5. YOUTH VS. ADULT FOOTBALL HELMETS . . . . .	37
5.1 Abstract . . . . .	37
5.2 Introduction . . . . .	37
5.3 Methods . . . . .	38
5.4 Results . . . . .	39
5.5 Discussion . . . . .	46
5.6 Acknowledgments . . . . .	47

	Page
6. 2018 FOOTBALL HELMET ROUNDUP . . . . .	48
6.1 Abstract . . . . .	48
6.2 Introduction . . . . .	48
6.3 Methods . . . . .	49
6.4 Results . . . . .	49
6.5 Discussion . . . . .	62
6.6 Acknowledgments . . . . .	64
7. CONCLUSIONS . . . . .	65
REFERENCES . . . . .	68
A. EXTRA FIGURES FROM 2018 FOOTBALL STUDY . . . . .	72

## LIST OF TABLES

Table	Page
2.1 Pneumatic ram impact location and velocity (m/s). Random locations are specified in a standard, and the Non-CG type hits refer to those which do not pass through the center of mass of the headform. . . . .	7
3.1 Parameter values in for B and in each cell with results from ANCOVA for the dimensionless translational acceleration parameter, $\Pi_1$ . The annotations, a, b, c, and d indicate significant ( $p < 0.05$ ) difference between unhelmeted Hybrid III, Full 90, 2nd Skull and Storelli Exoshield respectively.	21
3.2 Effect Size $\Pi_1$ compared from each device to the bare head. Largest effect size greater than 1 highlighted. . . . .	22
3.3 Statistical results from ANCOVA for the dimensionless angular acceleration parameter, $\Pi_2$ . The annotations, a, b, c, and d indicate significant ( $p < 0.05$ ) difference between unhelmeted Hybrid III, Full 90, 2nd Skull and Storelli Exoshield respectively. . . . .	23
3.4 Effect Size $\Pi_2$ compared from each device to the bare head. Largest effect size greater than 1 highlighted. . . . .	24
4.1 Parameter values in for A and in each cell with results from ANCOVA for the dimensionless translational acceleration parameter, $\Pi_1$ between types of headgear denoted with letters. The annotations, a, b, c, d, and e indicate significant difference ( $p < 0.05$ ) between the regression parameters of the unhelmeted Hybrid III, Schutt Stallion 650, Cascade CPX-R, Hummingbird and Cascade LX respectively. . . . .	30
4.2 Effect Size $\Pi_1$ compared from each device to the bare head. Largest effect size greater than 1 highlighted. . . . .	31
4.3 Parameter values in for A and in each cell with results from ANCOVA for the dimensionless translational acceleration parameter, $\Pi_2$ between types of headgear denoted with letters. The annotations, a, b, c, d, and e indicate significant difference ( $p < 0.05$ ) between the regression parameters of the unhelmeted Hybrid III, Schutt Stallion 650, Cascade CPX-R, Hummingbird and Cascade LX respectively. . . . .	32
4.4 Effect Size $\Pi_2$ compared from each device to the bare head. Largest effect size greater than 1 highlighted. . . . .	33

Table	Page
5.1 Parameter values in for $A$ and $\beta$ in each cell with results from ANCOVA for the dimensionless translational acceleration parameter, $\Pi_1$ between types of headgear denoted with letters. The annotations, a, b, c, d, and e indicate significant difference between unhelmeted Hybrid III, Riddell Speed Flex, Riddell Speed Flex Youth, Xenith Epic+ Youth and Xenith Epic+ respectively. . . . .	41
5.2 Parameter values in for $A$ and $\beta$ in each cell with results from ANCOVA for the dimensionless translational acceleration parameter, $\Pi_2$ between types of headgear denoted with letters. The annotations, a, b, c, d, and e indicate significant difference between unhelmeted Hybrid III, Riddell Speed Flex, Riddell Speed Flex Youth, Xenith Epic+ Youth and Xenith Epic+ respectively. . . . .	42
5.3 Effect size measures between each pair of helmets for the dimensionless translational acceleration, $\Pi_1$ . Highlights occur where a helmet is substantially different between the youth and adult versions. . . . .	43
5.4 Effect size measures between each pair of helmets for the dimensionless angular acceleration, $\Pi_2$ . Highlights occur where a helmet is substantially different between the youth and adult versions. . . . .	45
6.1 Parameter values in for $A$ and in each cell with results from ANCOVA for the dimensionless translational acceleration parameter, $\Pi_1$ between types of headgear denoted with letters. The annotations, a, b, c, d, e, f and g indicate significant difference ( $p < 0.05$ ) between the regression parameters of the unhelmeted Hybrid III, the Schutt Air XP Pro VTD II, the Vengeance VTD II, the Vengeance Pro, Xenith X2E+, Xenith Epic+, the Speed Flex, the Speed Icon, the Speed Classic, and the Vicis Zero 1. . . . .	51
6.2 Effect size measures between each helmet tested in the 2018 set relative to the bare head for the dimensionless translational acceleration, $\Pi_1$ . Largest effect size greater than 1 highlighted. . . . .	52
6.3 Effect size measures between each helmet tested in the 2018 set relative to the bare head for the dimensionless angular acceleration, $\Pi_2$ . Largest effect size greater than 1 highlighted. . . . .	53
6.4 Effect size measures between each Riddell helmet relative to the bare head for the dimensionless translational acceleration, $\Pi_1$ . Largest effect size greater than 1 highlighted. . . . .	55
6.5 Effect size measures between each Riddell helmet relative to the bare head for the dimensionless angular acceleration, $\Pi_2$ . Largest effect size greater than 1 highlighted. . . . .	56

Table	Page
6.6 Effect size measures between each Schutt helmet relative to the bare head for the dimensionless translational acceleration, $\Pi_1$ . Largest effect size greater than 1 highlighted. . . . .	58
6.7 Effect size measures between each Schutt helmet relative to the bare head for the dimensionless angular acceleration, $\Pi_2$ . Largest effect size greater than 1 highlighted. . . . .	59
6.8 Effect size measures between each Xenith helmet relative to the bare head for the dimensionless translational acceleration, $\Pi_1$ . Largest effect size greater than 1 highlighted. . . . .	61
6.9 Effect size measures between each Xenith helmet relative to the bare head for the dimensionless angular acceleration, $\Pi_2$ . Largest effect size greater than 1 highlighted. . . . .	62
A.1 Parameter values in for A and in each cell with results from ANCOVA for the dimensionless translational acceleration parameter, $\Pi_2$ between types of headgear denoted with letters. The annotations, a, b, c, d, and e indicate significant difference ( $p < 0.05$ ) between the regression parameters of the unhelmeted Hybrid III, the Schutt Air XP Pro VTD II, the Vengeance VTD II, the Vengeance Pro, Xenith X2E+, Xenith Epic+, the Speed Flex, the Speed Icon, the Speed Classic, and the Vicis Zero 1. . . . .	72

## LIST OF FIGURES

Figure	Page
2.1 An unhelmeted NOCSAE Drop Tower rig pictured in the HIRRT Laboratory and performed testing following the NOCSAE football helmet and lacrosse helmet testing from 2013. . . . .	4
2.2 The Hybrid III 50th Percentile Male headform and hydraulic ram rig from the 2019 NOCSAE Standard [FIGURE FROM [31]] . . . . .	5
2.3 The Hybrid III 50th Percentile Male headform and impulse hammer rig used by the HIRRT Lab for this work. Nine impact locations were used in the first study, each consecutive study utilized a slightly different location set, however many locations remained in common. For seven of the nine locations (Forehead = FH, Front Boss = FB, Side, Rear Boss = RB, Back, Top, and Facemask = FM), the blows were delivered approximately normal to the headform. For the other two locations, (Forehead-Oblique = FH-Obl, and Rear Boss-Oblique = RB-Obl), the impacts were administered at an oblique orientation of approximately 45°. [FIGURE FROM [40]] . . .	10
2.4 The impact administered was triggered when a force threshold reached 44N and was cutoff once the force fell below 44N. The time domain of time impact was determined, and the Impulse (Ns) was then calculated over it (A). The PF within this time domain was also determined. The accelerations measured by the Hybrid III headform were used to determine the PTA (B) from the translational acceleration (left) and the PAA from the angular acceleration (C). These peak values were calculated during and always occurred within the same time domain as was defined for the impact. (D) and (E) are the same impact with the trimmed time course from the during impact portion indicated by the impulse hammer. . . . .	11
2.5 Typical impacts to athletes measured by the xPatch (X2 Biosystems Inc, Seattle, WA) are qualitatively similar to the impacts recorded on the Hybrid III Headform (H3H) over a range of peak acceleration magnitudes. [FIGURE FROM [40]] . . . . .	13
2.6 Locations struck in the first round of impact tests. [FIGURE FROM [40]]	14
3.1 Impact location diagram describing the location of hits delivered to the soccer headgear. . . . .	19

Figure	Page
3.2 Front, Front-Oblique, Front Boss, and Side impact location data appear in A-D respectively . . . . .	20
3.3 Rear Boss, Rear Boss Oblique, and Rear impact location data appear in A-C respectively. . . . .	20
3.4 Front, Front-Oblique, Front Boss, and Side impact location data appear in A-D respectively . . . . .	23
4.1 Front, Front-Oblique, Front Boss, and Side impact location data appear in A-D respectively . . . . .	34
4.2 Rear Boss, Rear Boss Oblique, and Rear impact location data appear in A-C respectively. . . . .	34
4.3 Photos of the four helmets tested, from top to bottom and left to right, the Cascade LX, Hummingbird, Cascade CPXR, and Schutt Stallion 650. . . . .	35
5.1 Front, Front-Oblique, Front Boss, and Side impact location data appear in A-D respectively . . . . .	39
5.2 Rear Boss, Rear Boss Oblique, Rear, and Top impact location data appear in A-C respectively. impact location data appear in A-D respectively . . . . .	40
5.3 Front, Front-Oblique, Front Boss, and Side impact location data appear in A-D respectively . . . . .	40
5.4 Crack length visible on various helmets. A) is the Riddell Youth Speed Flex, B) and C) are the Xenith Epic+ Youth, D) is the Riddell Speed Flex, E) and F) are the Xenith Epic+ helmets. . . . .	44
6.1 Front, Front-Oblique, Front Boss, and Front Boss-Oblique impact location data appear in A-D respectively for the 2018 football helmets. . . . .	50
6.2 Side, Side-Oblique, Rear Boss, and Rear Boss-Oblique impact location data appear in A-D respectively for the 2018 football helmets. . . . .	50
6.3 Front, Front-Oblique, Front Boss, and Side impact location data appear in A-D respectively for the Riddell helmets tested with this methodology. . . . .	54
6.4 Front, Front-Oblique, Front Boss, and Side impact location data appear in A-D respectively for the Schutt helmets tested with this methodology. . . . .	57
6.5 Front, Front-Oblique, Front Boss, and Side impact location data appear in A-D respectively for the Xenith helmets tested with this methodology. . . . .	60
A.1 Rear, Rear-Oblique, Top, and Top-Oblique impact location data appear in A-D respectively for the 2018 football helmets. . . . .	73

Figure	Page
A.2 FR2, and FR2-Oblique impact location data appear in A and B respectively for the 2018 football helmets. . . . .	73
A.3 Rear Boss, Rear Boss Oblique, Rear, and Top impact location data appear in A-D respectively for the Riddell helmets tested with this methodology. .	74
A.4 Rear Boss, Rear Boss Oblique, Rear, and Top impact location data appear in A-D respectively for the Schutt helmets tested with this methodology. .	75
A.5 Rear Boss, Rear Boss Oblique, Rear, and Top impact location data appear in A-D respectively for the Xenith helmets tested with this methodology. .	76

## ABBREVIATIONS

CTE	Chronic Traumatic Encephalopathy
TBI	Traumatic Brain Injury
HAE	Head Acceleration Event
HIC	Head Injury Criterion
GSI	Gadd Severity Index
MRI	Magnetic Resonance Imaging
fMRI	Functional Magnetic Resonance Imaging
PTA	Peak Translational Acceleration
PAA/PRA	Peak Angular/Rotational Acceleration [Equivalent]
H3H	Hybrid III 50th Percentile Male Headform
CoM	Center of Mass
$a_p$	Peak Translational Acceleration
$\ddot{\Theta}_p$	Peak Angular Acceleration
$F_p$	Peak Force
$m_h$	Mass of Head
$m_T$	Mass of Head+Helmet
$W_n$	Width of Neck
$t_r$	Reference Time
$\Delta t$	Impact Duration
$\int F(t)dt$	Impulse
$L_n$	Length of Neck

## ABSTRACT

McIver, Kevin G. MSME, Purdue University, May 2019. Engineering Better Protective Headgear for Sport and Military Applications. Major Professor: Eric A. Nauman, School of Mechanical Engineering.

Recent applications of medical imaging, advanced polymers, and composites have led to the development of new equipment for athletes and soldiers. A desire to understand the performance of headgear that resists impacts ongoing since the 1970's has found more traction in recent years with the usage experimental models that have a greater degree of bio-fidelity. In order to determine which features of helmets from different sports (Soccer, Lacrosse, Football, and Hockey) were tested on a Hybrid III 50th Percentile Male headform with an accelerometer rig at the center of mass. Testing was performed by administering impacts to the headform with an impulse hammer that provides transient force data in order to quantify inputs and outputs of the system to develop a non-dimensional transfer function. Helmet performance is compared by sport worn in order to determine desirable manufacturing features and develop prototype helmets that outperforms current athletic equipment.

## 1. INTRODUCTION

Traumatic brain injuries (TBIs) are a class of pathology that that can cause profound detriments to the quality of life for individuals suffering from them which has been documented across numerous studies [1–5]. The earliest studies on this subject were from boxing, as early as 1927, changes were documented in people from repetitive head impacts and the term "Punch Drunk" was coined [6, 7]. Later studies theorized damage mechanisms that were unable to be confirmed without the invention of MRI and pathology studies that would come much later [8]. Later studies examined traumatic brain injuries in chimpanzees examining single impacts [9].

During 2010 there were 2.5 million TBI-related incidents that lead to hospitalizations, emergency room visits and deaths, which was 800,000 more cases than 2007 [10]. In the year 2010, TBI resulted in a net health care cost of an estimated \$76.5 billion between acute and long-term care [3, 11]. The rate of sports-related TBI has been estimated between 1.6 and 3.8 million cases per year, however recent ground-breaking studies demonstrated that only 14% of concussions are reported and/or diagnosed in a season of collegiate level football, which together could suggest as many as 27 million concussions occur per year [3, 12]. Recent work has also shown that persistent substantial physiological changes to the brain that last into the off-season can occur in the absence of symptoms in between 50 and 90% of athletes participating in high school football and women's soccer [13–21]. In football, helmets were first made mandatory use by the NCAA in 1939 to reduce the incidence of skull fracture; the first helmets were leather, and then plastic shells with chin straps were introduced in the early 1940s [22, 23]. Facemasks were originally added to these plastic shells in the mid-1950s.

The application of engineering techniques to improve helmets has not been heavily documented, and no rigorous procedure to quantify the ability of a helmet to

mitigate translational and angular accelerations has been developed. Prior work has developed a test rig utilizing a Hybrid III 50th percentile headform and an impulse hammer to measure the accuracy of accelerometers at the center of mass compared to the ear mounted sensors. The following chapters will cover the current standard criterion that were developed to attempt quantification of helmet performance, and then the development of a new framework whereby helmet performance can be compared relative to one another on the same stand in head-neck model.

While TBI due to blast injury is different than those caused by impacts, the principles developed in this thesis work can be applied to those injuries as well. Despite this thesis not covering a significant portion of blast injury or military applications, future work will entail applying the principles developed herein to advancing protective gear for servicemen as well.

Following the background chapter covering the methodology developed for this work, there are four experimental data sets that were collected wherein the same methods to test Soccer Headgear, Lacrosse Helmets, Youth vs. Adult Helmets and then a number of football helmets from the year 2018.

These studies were then used to illuminate the development of novel manufactured helmets that will be tested in order to show performance compared to current gear. This work is intended to guide the development of tailored headgear with quantification framework that can be applied to all sports and all levels of play. With this system, if typical impact force range and distribution data can be acquired for a given sport and level of play, helmet and padding systems can be developed to provide the most attenuation at the ranges seen at that level of play.

## 2. BACKGROUND

### 2.1 Current Methodologies

The development of criterion to specify performance of helmets and other headgear began in 1966 with the Gadd Severity Index (GSI) defined by,

$$GSI = \int_0^T \left(\frac{a}{g}\right)^{2.5} dt \quad (2.1)$$

where  $T$  is the impact duration and  $a$  is normalized by acceleration due to gravity, which must remain below a threshold determined from cadaver experiments [24]. In 1973, the National Committee on Operating Standards for Athletic Equipment (NOCSAE) introduced a drop tower test that was designed to certify football helmets for usage based on this criterion and reduced the incidence of fatalities [25]. Several others were developed, one of note is Versace's Head Impact Criterion which has two variants, one with a length of 15ms and one with a length of 36 ms that is commonly used in car crash evaluation,

$$HIC_{15} = (t_2 - t_1) \left[ \frac{1}{t_2 - t_1} \int_{t_1}^{t_2} (a(t))^{2.5} dt \right] \quad (2.2)$$

which takes into account only 15 ms of the acceleration [26,27]. NOCSAE does not allow the publication of SI results as a method to show one helmet outperforms another for any sport. Most helmets and headgear also seem to be designed for protection from massive trauma, and not protection from sub-concussive blows [28]. Though their original purpose was to mitigate skull fractures, the demonstrated physiological changes and clear long term risks of football and other contact and collision sports have been demonstrated via histological studies investigating the brains of numerous NFL players and suggest that new headgear needs to account for other factors than just skull fracture, and further that these changes should occur in other sports as well [29].

Current methodologies to standardize the testing of headgear have been attempted by the various national standards organizations, however none of the tests provide quantification for how headgear perform relative to one another. The 2013 standard NOCSAE helmet test utilized a drop tower (Figure 2.1).



Figure 2.1. An unhelmeted NOCSAE Drop Tower rig pictured in the HIRRT Laboratory and performed testing following the NOCSAE football helmet and lacrosse helmet testing from 2013.

This test is over-constraining, as it fails to account for angular acceleration to the headform, which is thought to play a large role in diffuse axonal injury patterns, and has been the center of attempts to model injury patterns from experimental data using ABAQUS [9, 30].

In order to model the process with more fidelity rigs utilizing Hybrid III 50th Percentile Male Head and Neck models and hydraulic or pneumatic rams (Figure 2.2) [31]. The ram test was first approved in January 2016, newly manufactured helmets were not required to meet the standard until November 2018, and prior to it the testing had remained the same since their inception in 1976. This test provides more biofidelity, but is still constrained by the accuracy of the Hybrid III 50th Percentile Male Head and Neck model for the human neck.

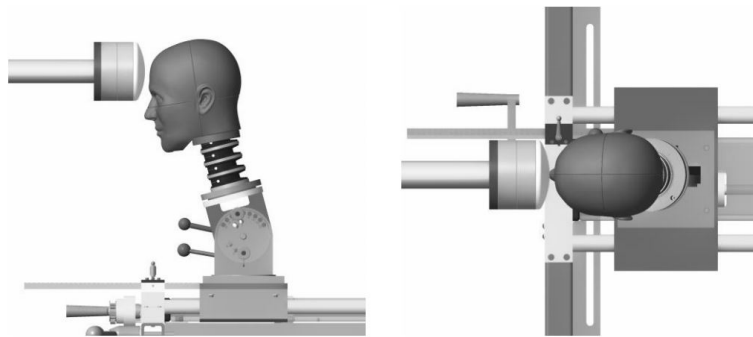


Figure 2.2. The Hybrid III 50th Percentile Male headform and hydraulic ram rig from the 2019 NOCSAE Standard [FIGURE FROM [31]]

In 2011 a team at Virginia Tech created the STAR rating system. The STAR system is an attempt to quantify "injury risk" using drop tower impacts and data collected from the HITS system [32]. The STAR rating is problematic to say the least, as it is fraught with errors and inconsistencies. The STAR tests are based on the standard NOCSAE drop test, and attempt to provide a qualified injury risk by quantification of impacts from data obtained from HITS system around country. Then it produces a function of risk based on a certain acceleration with magnitude

a. This is one of the biggest problems because it's difficult to say what magnitude causes damage.

Of particular note is that the studies that show the HITS system performs well are by the same group that created the STAR system, despite the fact that those studies utilized size Medium helmets on a 50th percentile male headform, which produces extremely high pressure on the surface of the headform that was beyond the 99th percentile of pressure on volunteer players [33]. Duma and Rowson responded with a letter to the editor in the Journal of Biomechanics in 2014, by saying that the testing performed by Jadischke et al. was not applicable to measure the accuracy of the HITS system because the hits were not representative of in-game collisions. Jadischke responded to Duma and Rowson's letter to the editor with his own, which related that the over 2 million head impacts recorded on the HITS system where the range of error for peak linear acceleration is between 0.4 and 40.8% error for shell impacts and 2.5-250% error for facemask impacts (from [33]). An additional flaw is that the HITS system has been shown by several researchers to perform quite poorly in setups with a 3-2-2-2 accelerometer array and a quantified force impact [34].

This new test protocol was faced with significant scrutiny, particularly from NOCSAE [35]. Ironically, NOCSAE criticized the STAR Rating system for not considering different sizes of helmets, as each helmet type was only tested in size Large, with the additional comment that Youth helmets were not tested, despite the fact that NOCSAE had also not performed or implemented tests which incorporated testing requirements for newly manufactured youth helmets. Additionally, NOCSAE stated that the STAR testing did not meet manufacturer specified fit conditions (which NOCSAE claims to apply) [35]. Only the most recent NOCSAE testing standard that went into effect November 2018 requires the usage of both the ram and the drop tower, both of which inputs are sent in terms of velocity, not in terms of the force of the impact or total impulse delivered [36]. Additionally, it is important to note that the new standard applies different testing requirements for youth and adult helmets, specifying lower impact velocities for the youth helmets (Table 2.1.

Table 2.1.

Pneumatic ram impact location and velocity (m/s). Random locations are specified in a standard, and the Non-CG type hits refer to those which do not pass through the center of mass of the headform.

Helmet Type	Side	Rear Boss (CG)	Rear Boss (Non-CG)	Rear	Front Boss	Random
Youth	5.2	5.2	5.2	5.2	5.2	5.2
Adult	6.0	6.0	6.0	6.0	6.0	6.0

These things taken together, suggest that no current test methodology for helmets has adequately quantified performance of helmets to identify those design features which should be incorporated to best protect players in various sports that examines headgear with quantified inputs and outputs that does not claim to assess the risk of concussion. To assess the design of a better helmet it is critical that longitudinal studies with high populations of players assessing total neurological health with respect to pre-season, in-season, and post-season MRI, fMRI, and neurological assessments to determine whether long-term changes due to repetitive subconcussive impacts are being reduced rather than just individual concussive blows.

## 2.2 A Non-Dimensional Framework to Assess the Performance of Helmets in Sport and Military Applications

*Material found in this section has appeared in Cummiskey, Sankaran, and McIver et al. 2019*

This has motivated an examination of several helmet types that will be covered in this thesis, from football helmets, to soccer headgear, to lacrosse helmets, as well as hockey helmets and the manufacturing of new prototypes. With respect to football helmets youth and adult helmets of the same brand and model were also compared. It is important for future work to apply these principles to improve the ability of military helmets to reduce traumatic brain injury from physical hits, as well as influ-

encing future work regarding the reduction of physiological damage from secondary neurotrauma from blasts in vehicles.

### 2.2.1 Theory

There are a number of limitations associated with the usage of GSI as a measure of helmet performance within the context of NOCSAE-style tests. The most important limitation is that the criterion are only based on output measures of head acceleration in response to a few severe-loading conditions as opposed to relating the input loads to the output acceleration. Without a transfer function between the inputs and outputs it is difficult to identify which features of helmet design mitigate the impacts across a wide spectrum of potentially injurious head blows. It should be noted that empirical modeling with experiments is critical because determining the equations that govern the deformation of the helmet's shell and padding, the forces at the interface, and the motion of the head and neck is extremely difficult.

In addition, the GSI normalizes the measured accelerations by the acceleration due to gravity. The method provides a useful context for comparing PTA to PTA, but does not appear in the dimensional analysis simply because gravitational potential energy is not a factor in these types of HAEs. A proper normalization requires consideration of both the input and output variables normalized by the factors that influence the head response [37]. To develop a comprehensive set of parameters, dimensionless groups were developed to relate the output measures of interest: the peak translational acceleration (PTA),  $a_p$ , and the peak angular acceleration (PAA),  $\ddot{\Theta}_p$  to the primary input parameters: mass of the head  $m_h$ ; width of the neck  $W_n$ ; the difference,  $(t_r - \Delta t)$ , between a reference time  $t_r = 100\text{ms}$ , and the impact duration  $\Delta t$ ; the impulse delivered to the head,  $\int F(t)dt$ , where  $F(t)$  was the time-varying impact force; total combined mass of the head and helmet,  $m_T$ ; and the neck length,  $L_n$  [38, 39]. Because there are three relevant dimensions, mass, length, and time,

three parameters ( $m_h$ ,  $w_n$ , and  $t_r \cdot \Delta t$ ) were chosen to nondimensionalize the output variables and the remaining input variables according to the Buckingham Pi theorem.

This framework was first published in Cummiskey 2019 after three years of development, data collection, analysis, and fine tuning. The mathematical model was developed utilizing intermediate asymptotics and non-dimensionalization [40].

Ultimately,  $\Pi_3$  and  $\Pi_4$  were discarded from the analysis prior to publication in favor of  $\Pi_1$  and  $\Pi_2$  which separated performance better. Inputs:

$$\Pi_1 = \frac{a_p * (\Delta t)^2}{W_n} \quad (2.3)$$

$$\Pi_2 = \ddot{\Theta}(\Delta t)^2 \quad (2.4)$$

$$\Pi_3 = \frac{\int a * \Delta t}{W_n} \quad (2.5)$$

$$\Pi_4 = \int \ddot{\Theta}(\Delta t) \quad (2.6)$$

Outputs:

$$\pi_1 = \frac{\int F dt * (\Delta t)}{W_n * m_h} \quad (2.7)$$

$$\pi_2 = \frac{m_T}{m_h} \quad (2.8)$$

$$\pi_3 = \frac{L_n}{W_n} \quad (2.9)$$

$$\pi_4 = \frac{R_T}{W_n} \quad (2.10)$$

These non-dimensional equations are then combined into an intermediate asymptotic model [37] to relate each output variable  $\Pi_j$  where the subscript  $j = 1$  or  $2$  to the input parameter yields an equation of the form

$$\Pi_j = B_j \pi_1^{\beta_{1j}} \pi_2^{\beta_{2j}} \pi_3^{\beta_{3j}} \quad (2.11)$$

The full process of statistical analyses performed will be discussed after the data collection is described in detail.

### 2.2.2 Data Collection

Impacts were administered to each helmet and the unhelmeted headform using a modally tuned impulse hammer (PCB Piezotronics, Inc.; Depew, NY; see Figure 2.3) with a 5 cm diameter face as described by Cummiskey et al. utilizing the "Super Soft Gray Plastic Hammer Tip" which gave impact durations most like those seen in the X2 on-field data [34].

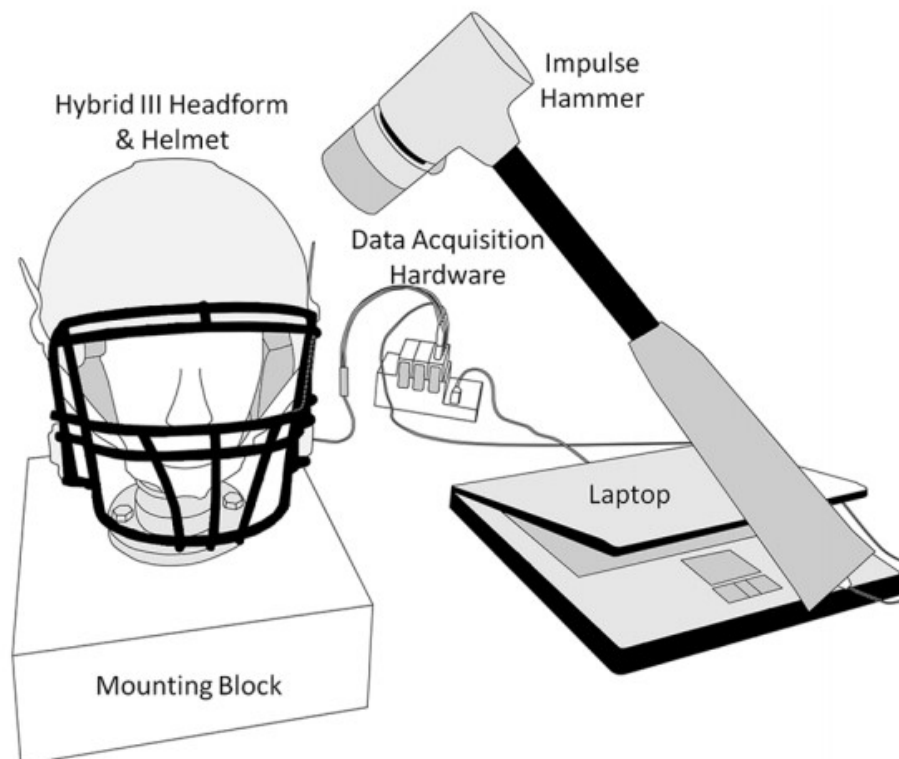


Figure 2.3. The Hybrid III 50th Percentile Male headform and impulse hammer rig used by the HIRRT Lab for this work. Nine impact locations were used in the first study, each consecutive study utilized a slightly different location set, however many locations remained in common. For seven of the nine locations (Forehead = FH, Front Boss = FB, Side, Rear Boss = RB, Back, Top, and Facemask = FM), the blows were delivered approximately normal to the headform. For the other two locations, (Forehead-Oblique = FH-Obl, and Rear Boss-Oblique = RB-Obl), the impacts were administered at an oblique orientation of approximately 45°. [FIGURE FROM [40]]

During each impact, the transient force data measured at the face of the hammer caused an impact event to be generated whenever the force went above a threshold of 10 lbf (44N) (Figure 2.4).

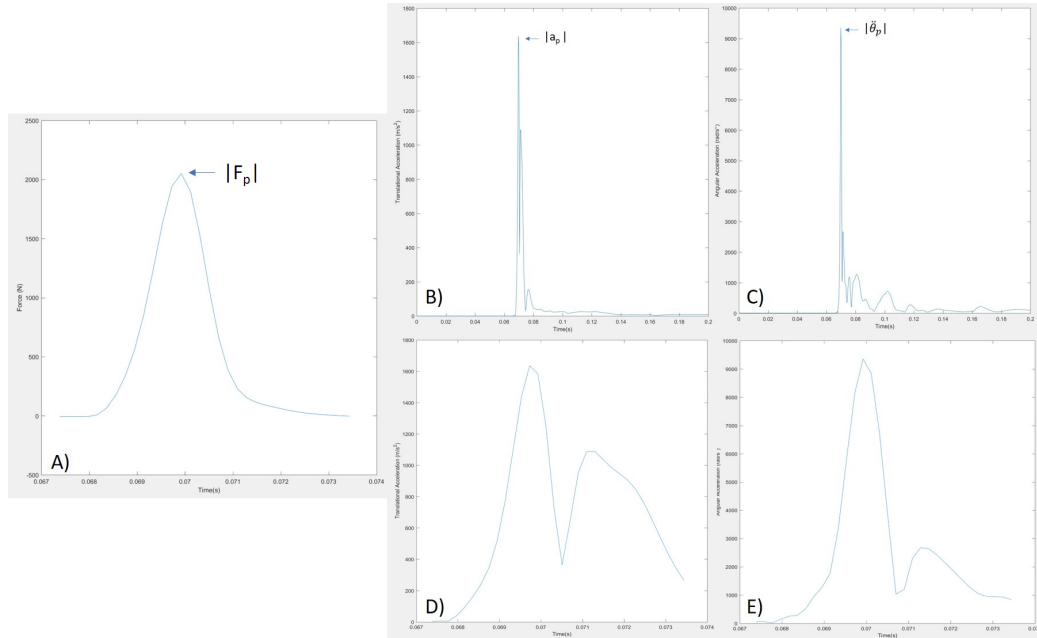


Figure 2.4. The impact administered was triggered when a force threshold reached 44N and was cutoff once the force fell below 44N. The time domain of time impact was determined, and the Impulse (Ns) was then calculated over it (A). The PF within this time domain was also determined. The accelerations measured by the Hybrid III headform were used to determine the PTA (B) from the translational acceleration (left) and the PAA from the angular acceleration (C). These peak values were calculated during and always occurred within the same time domain as was defined for the impact. (D) and (E) are the same impact with the trimmed time course from the during impact portion indicated by the impulse hammer.

During each impact event, nine accelerometers (one triaxial and six uniaxial) housed inside of the Hybrid III headform using the 3-2-2-2 configuration produced translational and rotational acceleration traces for the Hybrid III headform center of mass [34, 40, 41]. Model 9234 data acquisition modules (NI; Austin, TX) in an NI cDAQ 9174 base were used to measure all 10 channels of data over coinciding

time domains, and control of the hardware was accomplished using a custom software package written in LabView 2014. Data were sampled at 5120 Hz, well above the Nyquist rate of these impacts.

The LabView package save raw data for each impact, filters the acceleration traces using a low-pass Butterworth filter with a cutoff frequency of 750Hz, then kinematically determines the resultant translational and angular acceleration at the center of mass and compiles those data, along with the non-dimensional parameters for each impact into a final Output sheet that is passed to a custom MATLAB code that performs the statistical analyses, which will be discussed after the data collection methodology. Impacts delivered with the modal hammer provided good representations of the impacts typically experienced by football players during practices and games as determined in previous studies (Figure 2.5) [34, 40].

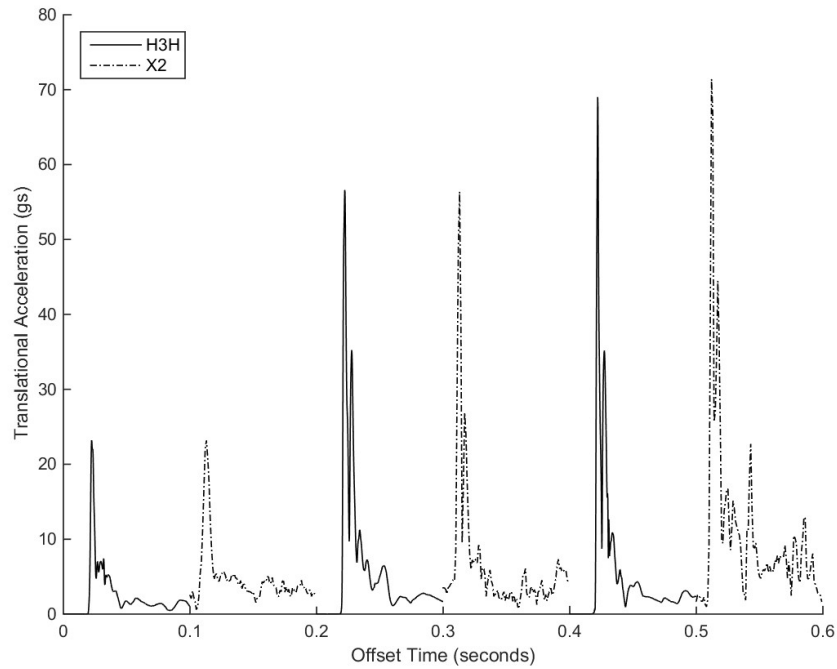


Figure 2.5. Typical impacts to athletes measured by the xPatch (X2 Biosystems Inc, Seattle, WA) are qualitatively similar to the impacts recorded on the Hybrid III Headform (H3H) over a range of peak acceleration magnitudes. [FIGURE FROM [40]]

After testing, the helmets were visually inspected for signs of damage including permanent deformations of the facemask, cracks, and delamination. Helmets were struck at a variety of locations, hit locations for the first study are included in (Figure 2.6).

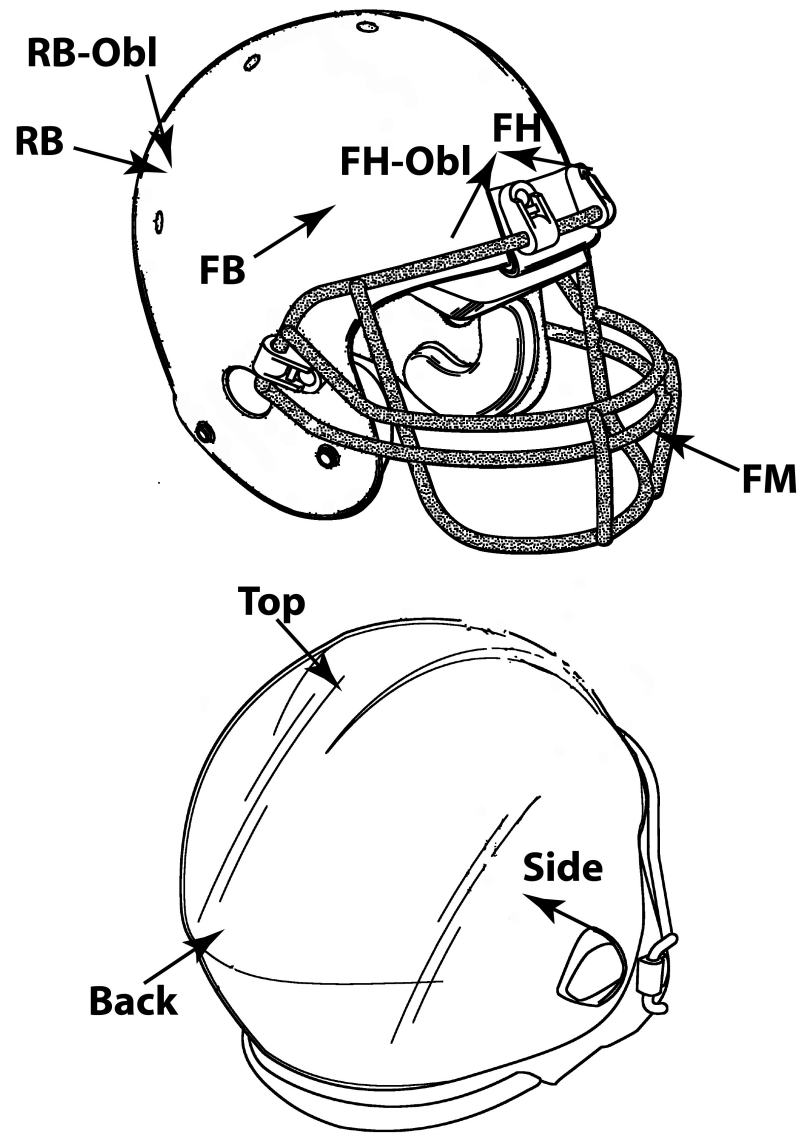


Figure 2.6. Locations struck in the first round of impact tests. [FIGURE FROM [40]]

### 2.2.3 Statistical Analysis

Each testing set was performed on the Hybrid III Test Rig, which removes Eqns. 2.9 and 2.10 from the fit model as they do not vary in any analysis. Eqn. 2.8

is also removed from consideration for the chapters including the Soccer Headgear, Lacrosse Helmets, and Youth Vs. Adult Helmets, as the helmet mass does not vary substantially between helmets analyzed. This leaves a two parameter equation, and log transformation after removal of terms from Eqn. 2.11 leaves a simple linear regression given by,

$$\ln(\Pi_j) = \ln(B_j) + \beta_{1j}\ln(\pi_1) \quad (2.12)$$

A custom MATLAB code for post-processing used a modification of Grubbs' method to remove outliers from the data set. A preliminary curve fit was generated utilizing Eqn. 2.12 and an estimate of the standard deviation was obtained by calculating the square of the difference between each data point, and the point on the curve fit, dividing by  $n-1$  and taking the square root of the result. Points more than 3 standard deviations from the curve fit equations were removed from the data set. After each point was checked, the final curve fit was performed on the reduced data set to obtain the final parameter values. In each analysis no more than 8/60 points were removed (including those hits deemed invalid due to acceleration spike errors from wires jostling in the electromechanical system).

Subsequently, the regression coefficients for the unhelmeted headform and each helmet were statistically evaluated for significant differences using an analysis of covariance (ANCOVA) test with an  $\alpha$  level of 0.05. To compare the differences found in the ANCOVA test, a Tukey post-hoc test with a Holm-Sidak p-value correction was utilized [40]. The regression coefficients were utilized with the intermediate asymptotic fit model to determine the effect size between the helmets and the bare head at 100 evenly spaced values spanning the distance between the minimum and maximum values of  $\pi_1$  and averaged for each location. The effect size calculation provided a measure of the average difference between groups relative to the variability of the overall measurements.

This entire process was designed to develop a rigorous approach to quantification of performance in hard measures. With this methodology reduction of the PTA and

PAA of a given blow to the head across a large number of impact ranges to ensure helmets protect from low-level impacts that are seen on every play and extreme impacts beyond the 99th percentile of impacts in the sport. The remainder of the thesis will examine the effectiveness of this tool at analyzing the ability of different headgear to attenuate HAEs.

### 3. SOCCER HEADGEAR

*Material found in this chapter has or will appear in a journal publication*

#### 3.1 Abstract

Long-term neurocognitive deficiency due to subconcussive impacts is a concern for athletes who participate in combat, collision, and contact sports. Football players wear helmets that can help reduce injury risks like skull fractures, and these helmets must meet standard criteria. Currently no standard exists for testing soccer headgear despite studies demonstrating soccer players experience similar impact magnitudes. In this study, a modal impact hammer was used in conjunction with a Hybrid III 50th percentile male headform to simulate impacts experienced by soccer players to quantify the effectiveness of headgear in attenuating head impacts. The study found that devices were minimally effective at reducing the non-dimensional translational parameter substantially at the front, front oblique, or front boss impact locations, providing no real change in translational acceleration that would be experienced during a header. This study also found that no device caused a substantial reduction in the non-dimensional angular acceleration parameter at any location, suggesting that there is room for substantial improvement in device design. Devices need to be developed and common testing standards need to be established to allow for a more widespread implementation of similar devices to protect players from short and long-term injuries due to head impacts.

#### 3.2 Introduction

As far as various sports besides football are concerned, soccer is the leading cause of concussions among female athletes for a variety of reasons, with the particular act of

heading the ball causing approximately 40.5% of all concussions in boys' soccer [42,43]. Neither NOCSAE, ASTM, nor ISO certify headgear for usage in soccer. National and international federations do not enforce or endorse the usage of protective headgear in soccer. Despite the lack of mandate for headgear, it has previously been shown that college women sustain similar blows to those playing football, and greater numbers than their high school female soccer player counterparts [44].

This study seeks to determine the efficacy various types of headgear at attenuating the resultant translational and angular acceleration from impacts experienced by soccer players. In this study, we investigated the impact attenuation properties of 2nd Skull 5mm headbands (2nd Skull; Pittsburgh, PA), Full 90 headbands (Full 90; San Diego, CA) and Storelli Exoshield Headbands (Storelli; Brooklyn, NY). These devices were compared with the performance of the unadorned 50th Percentile Hybrid III headform (H3H). An impulse hammer was used to administer impacts along the headform at seven test locations on 3 different samples of each device tested [34,40]. Withnall et al. utilized two Hybrid III testing rigs in two orientations to test the viability of the Full 90 among other types of headgear on a drop rig and found it to be ineffective at reducing impact from ball contact, yet found that in cases of head to head contact some devices could provide a measure of protection [45]

### 3.3 Methods

The study was designed to test the effectiveness of three different types of soccer headgear, the 2nd Skull, Full 90 and Storelli Exoshield headbands in reducing the accelerations experienced by the head when struck in soccer. In the test cases, the head gear was fitted to the H3H testing rig, after which the head gear was struck repeatedly at seven different locations (Figure 3.1). The 20 impacts at each of the impact locations were divided into five distinct impulse ranges, 2-4 Ns, 4-7 Ns, 8-10 Ns, 11-12 Ns and 13-14 Ns (which were then collected 4 times each. This range simulates a range of hits well over the 90th percentile (71.2 g) with a maximum acceleration near

180 gs with the intent of replicating those hits that are most dangerous to players [44]. The testing was post-processed utilizing the same methodology previously discussed in the Background Chapter.

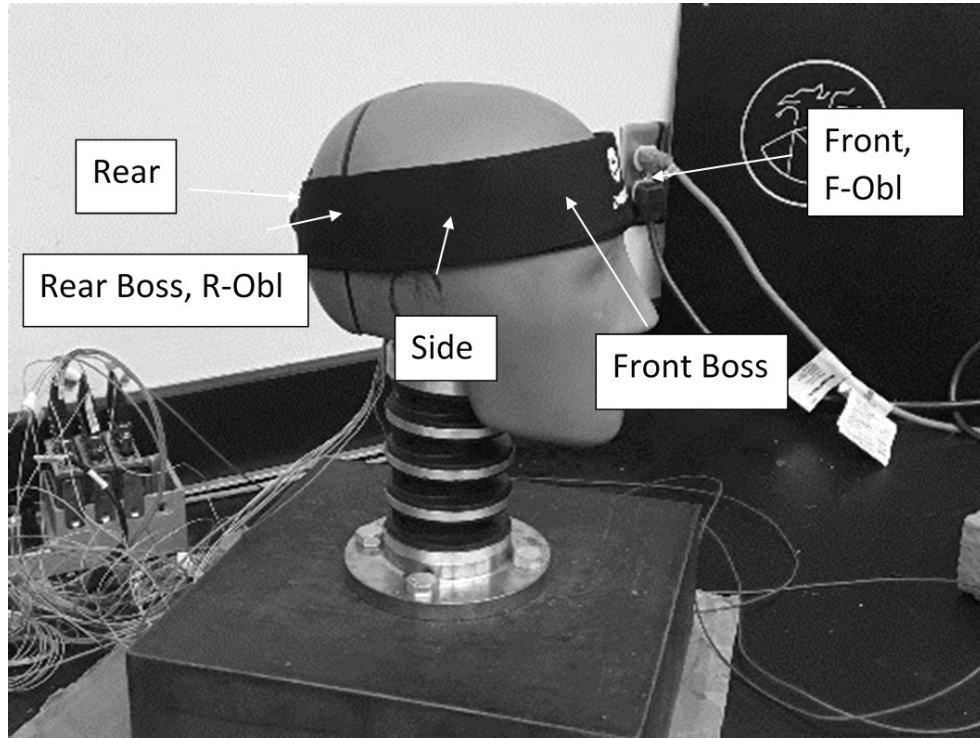


Figure 3.1. Impact location diagram describing the location of hits delivered to the soccer headgear.

### 3.4 Results

The 2nd Skull headbands are composed of a proprietary foam with a spandex/nylon sheathe, and the Full 90 is another type of proprietary foam padding, as is the Storelli. The Full 90 headbands had a mass of .0687 kg, while the 2nd skull headbands had a mass of .026 and .045 for the 2mm and 5mm versions respectively. The Storelli Exoshield has a mass of .107 kg. The curve fits for each parameter of interest were determined with the MATLAB code and then graphed (Figures 3.2, 3.3).

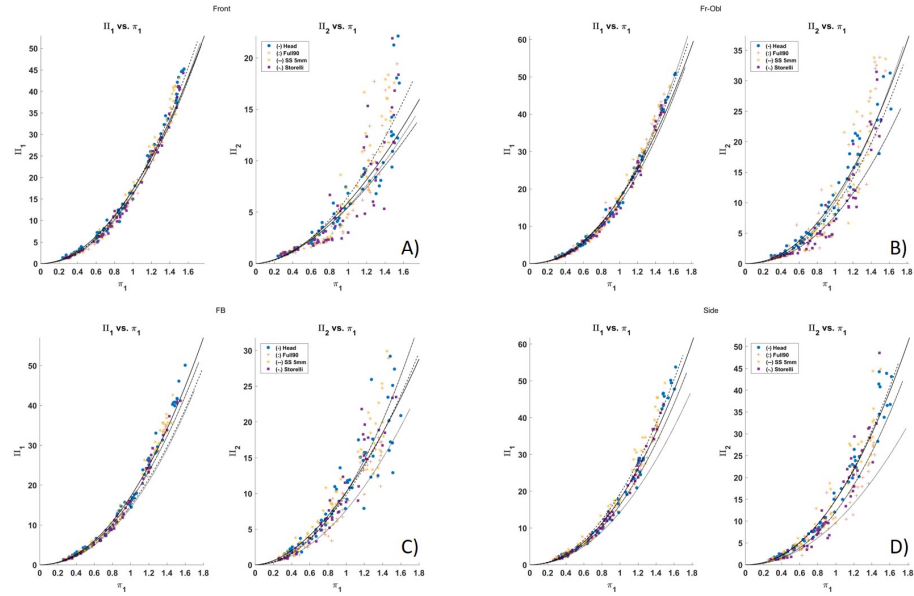


Figure 3.2. Front, Front-Oblique, Front Boss, and Side impact location data appear in A-D respectively

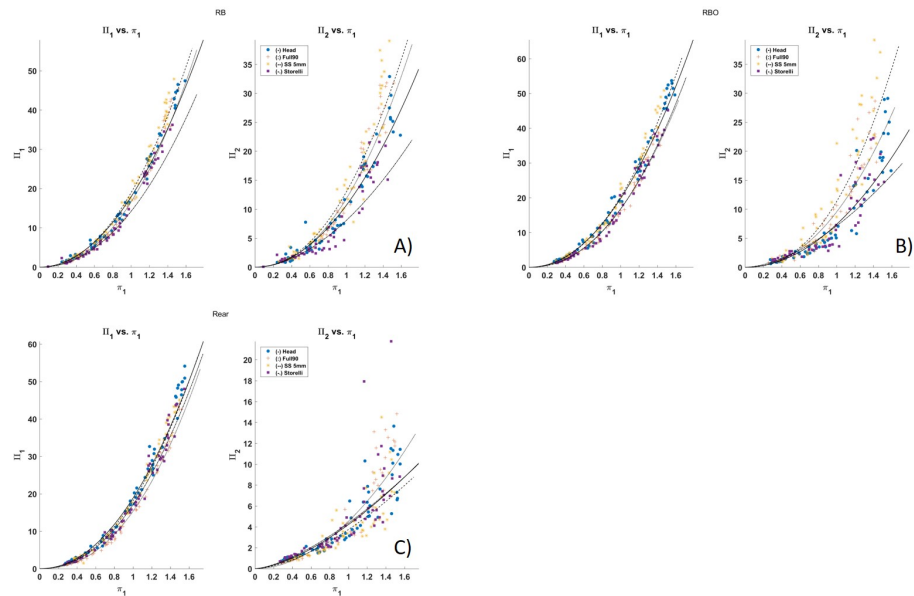


Figure 3.3. Rear Boss, Rear Boss Oblique, and Rear impact location data appear in A-C respectively.

The regression coefficients for the first parameter of interest, peak translational acceleration, at each location were calculated (Table 3.1). An effect size calculation was done to compare how large the difference between the dimensionless output functions were when compared to the bare head equation. An effect size of greater than one is considered to be a substantial reduction. For the translational non-dimensional parameters, the Storelli Exoshield provided an effect size of just over 1 at the Rear Boss and Rear Boss Oblique locations, with the Full 90 provided an effect size of 1.17 at the rear boss oblique and 1.31 at the rear location with all other locations providing an insubstantial reduction (Table 3.2).

Table 3.1.

Parameter values in for B and  $\beta_{1i}$  in each cell with results from ANCOVA for the dimensionless translational acceleration parameter,  $\Pi_1$ . The annotations, a, b, c, and d indicate significant ( $p < 0.05$ ) difference between unhelmeted Hybrid III, Full 90, 2nd Skull and Storelli Exoshield respectively.

		<b>Locations</b>						
		<b>1</b>	<b>2</b>	<b>3</b>	<b>4</b>	<b>5</b>	<b>6</b>	<b>7</b>
<b>Hybrid III</b>	$B_1$	17.54 (bcd)	17.31 (bd)	17.14	17.87	17.92 (bcd)	19.81 (bcd)	18.85 (bcd)
	$\beta_{1i}$	1.96 (bcd)	2.06 (bcd)	2.04	2.07	2.02 (bc)	2.05 (bcd)	2.08 (bd)
<b>Full 90</b>	$B_1$	15.96 (acd)	17.52 (ad)	16.47	17.08	16.62 (acd)	16.75 (ac)	15.34 (acd)
	$\beta_{1i}$	2.13 (ad)	2.21 (a)	2.10	2.05	2.22 (acd)	2.15 (a)	2.30 (acd)
<b>2nd Skull 5mm</b>	$B_1$	17.17 (abd)	17.39 (d)	17.17	19.28	18.96 (abd)	20.28 (abd)	18.17 (abd)
	$\beta_{1i}$	2.07 (a)	2.16 (a)	2.06	2.04	2.11 (ab)	2.13 (a)	2.16 (b)
<b>Storelli Exoshield Head Guard</b>	$B_1$	16.24 (abc)	16.53 (abc)	16.13	17.44	15.41 (abc)	16.78 (ac)	17.12 (abc)
	$\beta_{1i}$	2.05 (ab)	2.16 (a)	2.05	2.10	2.09 (b)	2.19 (a)	2.16 (ab)

Table 3.2.

Effect Size  $\Pi_1$  compared from each device to the bare head. Largest effect size greater than 1 highlighted.

	Full 90	SS 5mm	Storelli Exoshield
Forehead	0.79	0.21	0.60
Forehead Oblique	0.48	0.30	0.33
Front Boss	0.33	0.04	0.54
Side	0.33	0.48	0.17
Rear Boss	0.42	0.49	1.03
Rear Boss Oblique	1.07	0.26	1.11
Rear	1.25	0.22	0.57

The coefficients according to the model were also calculated at each location for the second parameter of interest, peak angular acceleration (Table 3.3). For the angular parameters, the Storelli Exoshield provided an effect size of 1.51 at the Forehead Oblique, the Full 90 provided an effect size of 1.48 at the Side and the SS 5mm provided an effect size of 1.09 at the Rear Boss Oblique, with all other locations providing an insubstantial reduction (Table 3.4).

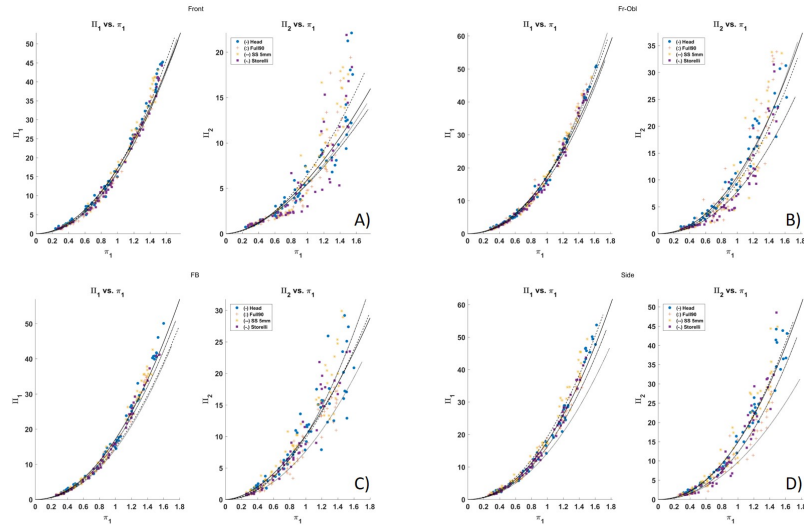


Figure 3.4. Front, Front-Oblique, Front Boss, and Side impact location data appear in A-D respectively

Table 3.3.

Statistical results from ANCOVA for the dimensionless angular acceleration parameter,  $\Pi_2$ . The annotations, a, b, c, and d indicate significant ( $p < 0.05$ ) difference between unhelmeted Hybrid III, Full 90, 2nd Skull and Storelli Exoshield respectively.

		Locations						
		1	2	3	4	5	6	7
<b>Hybrid III</b>	$B_2$	6.05	10.65	10.16 (bc)	14.82	10.69 (bcd)	7.43 (bcd)	4.22 (bc)
	$\beta_{1i}$	1.73	2.09	1.77 (bd)	2.10	2.00 (b)	1.99 (cd)	1.56 (b)
<b>Full 90</b>	$B_2$	5.54	10.11	8.74 (acd)	11.53	11.86 (acd)	9.60 (acd)	4.53 (ac)
	$\beta_{1i}$	1.73	2.23	1.97 (a)	2.04	2.18 (ad)	2.16 (cd)	1.94 (acd)
<b>2nd Skull 5mm</b>	$B_2$	6.51	9.38	11.14 (abd)	14.89	13.02 (abd)	11.39 (abd)	3.74 (abd)
	$\beta_{1i}$	1.89	2.21	1.90 (d)	2.14	2.16 (d)	2.35 (abd)	1.61 (b)
<b>Storelli Exoshield Head Guard</b>	$B_2$	5.46	8.02	10.10 (bc)	13.05	8.69 (abc)	7.15 (abc)	4.36 (c)
	$\beta_{1i}$	1.65	2.15	2.05 (ac)	2.24	1.85 (bc)	1.70 (abc)	1.49 (b)

Table 3.4.  
Effect Size  $\Pi_2$  compared from each device to the bare head. Largest effect size greater than 1 highlighted.

	Full 90	SS 5mm	Storelli Exoshield
Forehead	0.18	0.21	0.20
Forehead Oblique	0.11	0.33	0.76
Front Boss	0.41	0.28	0.26
Side	0.95	0.05	0.40
Rear Boss	0.48	0.63	0.61
Rear Boss Oblique	0.50	0.84	0.17
Rear	0.29	0.21	0.05

### 3.5 Discussion

This study was intended to related impulse delivered to the headform-headband system to the resultant components of acceleration to generate a transfer function to compare those relations between different headgear and assess effectiveness. The intermediate asymptotics relationship used provided the curve fitting parameters for the statistical comparisons. The ability to mitigate these impacts varied significantly between devices. Thickness of the devices tested relates very well with the attenuation of acceleration as these devices, unlike football helmets, have no outer shell that can deform and consist solely of sheathed padding. The padding attenuates energy only by compression, and provides no other methods to dissipate energy. This study showed that for the average magnitude hit for female soccer players (approximately 37g's) none of the helmets provided a substantial reduction according to effect size calculations at the front impact region [44].

For translational acceleration, these devices provided no large reductions as measured by the effect size in the magnitude of acceleration for Forehead, Forehead Oblique, Front Boss or the Side locations. There were some reductions seen at the Rear Boss, Rear Boss Oblique and Rear locations, but these were not very large reductions. Prior studies with football helmets have shown effect sizes from 3-4 in this mathematical model, whereas the largest seen here was 1.31 at the Rear from the Full 90 [34]. Angular acceleration showed only sporadic reductions with each device providing one effect size greater than 1 at three different locations. The largest effect size seen in these devices was 1.51. It should be noted that no device reduced the angular accelerations at the forehead, which is troublesome particularly in soccer where some of the largest impacts come from planned headers performed in soccer. No current standard of testing exists for these devices. Additionally, no test, including the NOCSAE standard tests for football helmets, can predict whether a device like this is functional enough to prevent physiological changes due to subconcussive blows. A prior study has shown a high hit group and a low hit group, and headgear like this, if functional could work to remove players from that high hit group [21].

In conclusion, this study used a similar methodology to produce an intermediate asymptotic transfer function through the use of carefully quantified system inputs and outputs. It was possible to statistically quantify the attenuation of acceleration at each tested location and determine an effect size for each headgear to determine mathematically which one provides the largest reduction. This methodology provides a design tool that can serve as a benchmark for testing of soccer headgear aimed at reducing the severity of impacts experienced by athletes in soccer. To truly determine if a helmet design is good enough requires careful imaging of brain structure, function and chemistry to quantify any changes seen over the course of a players season to prevent any changes due to subconcussive blows. The framework herein provides a comprehensive design tool that can serve as a benchmark for soccer headgear testing aimed at reducing the severity of impacts experienced by athletes in soccer. No particular headgear has been shown to reduce the damage accrued in any contact or

collision sport. Studies much like those performed by Purdue Neurotrauma Group, with pre-season, in-season, and post-season fMRI and MRS must be combined with tracking of HAEs experienced by players in a given sport wearing specifically chosen headgear in order to confirm the effect.

## 4. LACROSSE HELMETS

*Material found in this chapter has or will appear in a journal publication*

### 4.1 Abstract

It has been established that substantial negative changes in neurocognitive function can be observed in a large percentage of athletes who participate in contact sports such as soccer or football, motivating a need for improved safety systems. Previous studies have sought to evaluate the ability of modern football helmets to mitigate impacts both normal and oblique to the surface of the helmet using a system that quantifies both the input load and the resulting accelerations of a Hybrid III headform. This study quantifies the transfer function connecting inputs and outputs of the system to provide a comparison of the impact attenuation capability of male and female lacrosse helmets to reduce acceleration on the Hybrid III headform. Of those helmets tested, the better performing male helmet was the Schutt Stallion 650. With consideration to the fact that women's lacrosse is a non-contact sport, the Hummingbird performs best, however it should be noted that the device failed to survive the impacts in testing.

### 4.2 Introduction

Lacrosse is one of the fastest growing contact sports in North America, and head injury is a significant risk [42, 46]. Both laboratory and on-field studies have demonstrated average peak translational accelerations similar to those experienced in American football and womens soccer [47, 48]. Womens lacrosse ranks just behind American football with regard to the incidence rate of concussions and female players have a higher incidence of head, face and eye injury than men [42]. In light of recent

work demonstrating that substantial physiological changes can occur without symptoms in athletes that play high school football and soccer, these data suggest that mechanisms for reducing the magnitude of head impacts in lacrosse deserves further investigation [13, 17, 19, 20]. In order to mitigate the effects of head impacts, in 1973 the National Committee on Operating Standards for Athletic Equipment (NOCSAE) created a drop tower-based criterion to certify football helmets which reduced the incidence of fatalities [25, 26]. Similar standards introduced for Lacrosse helmets demonstrated that football helmets far outperformed those used in mens lacrosse, led to recalls and called into question effects of refurbishing [49]. Vollavanh et al. found average head accelerations in men’s lacrosse are similar to those that are in football and women’s soccer and further studies showed that most (78%) of the hits come to the front and sides [47, 48]. The NOCSAE standard was most recently updated in February 2018 and currently calls for the use of linear pneumatic rams to apply impact loads [50]. In addition, United States Lacrosse requires womens helmets to follow ASTM Safety Standard F3137-15, which specifies that helmet shells must remain flexible to protect unhelmeted players and also uses typical drop systems for testing [51]. The overall goal of this study was to evaluate the ability of mens and womens lacrosse helmets to mitigate the effects of head impacts using a common, modal hammer-based protocol that quantifies both the input load and output accelerations [34].

### 4.3 Methods

The study was designed to test the effectiveness of two helmet models designed for mens lacrosse the Schutt Stallion 650 (Schutt Sports; Litchfield, IL), and the Cascade CPX-R (Cascade; Liverpool, NY) and two helmet models designed for womens lacrosse the Hummingbird (Hummingbird Sports; Holmdel, NJ), and the Cascade LX (Cascade; Liverpool, NY). The mass of each helmet was measured three times and averaged to minimize error. The Schutt Stallion 650 had a mass of 1.426kg, the Cas-

cade CPX-R had a mass of 1.109kg, the Hummingbird had a mass of 0.728kg, and the Cascade LX was the lightest helmet at 0.609kg. Subsequently, the helmet was struck repeatedly at seven different locations. A 200 ms time series was collected for each normal and oblique impact with a 70 ms pre-trigger, providing 130 ms of acceleration and impact force measurements. The 20 impacts at each location were equally divided into five distinct impulse ranges from 2-4Ns, 5-7Ns, 8-10Ns, 11-13Ns, 14+Ns. Each helmet model was tested in triplicate for a total of 420 measurements per protective device to correct for any systematic errors that may result from a defect in a single device. During testing, the Hummingbird helmet suffered from significant damage from impacts to the Rear Boss and Rear Boss Oblique, leading to 10 missing measurements at Rear Boss, and 40 at the Rear Boss Oblique. Further, no data were collected at the Rear test location for this helmet.

#### 4.4 Results

Relative to the unhelmeted Hybrid III, each of the helmets significantly reduced the dimensionless translational acceleration at each of the impact locations, with the caveat that we were unable to successfully test the Rear location of the Hummingbird (Table 4.1). The Cascade CPX-R had the lowest  $\lambda$  values at the first three locations, with the Schutt Stallion 650 having the lowest values at the last four test locations although there was no significant difference in the  $\lambda$  values between the two helmets at the Front-Oblique and Front Boss locations. When comparing the effect size between helmets and the bare head, the Schutt Stallion provided the most substantial reduction from the bare headform from the Front-Oblique location through testing at the Rear Boss (Table 4.2). The Hummingbird exhibited the most substantial effect size at the rear boss oblique location.

Table 4.1.

Parameter values in for A and  $\beta_1$  in each cell with results from ANCOVA for the dimensionless translational acceleration parameter,  $\Pi_1$  between types of headgear denoted with letters. The annotations, a, b, c, d, and e indicate significant difference ( $p < 0.05$ ) between the regression parameters of the unhelmeted Hybrid III, Schutt Stallion 650, Cascade CPX-R, Hummingbird and Cascade LX respectively.

Locations								
		Front	Front-O	Front Boss	Side	Rear Boss	Rear Boss-O	Rear
<b>Hybrid III</b>	$A_1$	17.54 (bcde)	17.31 (bcde)	17.14 (bcde)	17.87 (bcde)	17.92 (bcde)	19.81 (bcde)	18.85 (bce)
	$\beta_1$	1.96 (bcde)	2.06 (bcde)	2.04 (bce)	2.07 (bce)	2.02 (bce)	2.05 (bce)	2.08 (bce)
<b>Schutt Stallion 650</b>	$A_1$	8.89 (acde)	8.23 (acde)	7.22 (acde)	7.60 (acde)	7.65 (acde)	7.49 (acde)	6.36 (ace)
	$\beta_1$	1.55 (acde)	1.53 (ade)	1.46 (ade)	0.88 (acde)	0.94 (acde)	1.06 (acde)	1.14 (ace)
<b>Cascade CPX-R</b>	$A_1$	7.03 (abe)	6.73 (abde)	6.72 (abde)	8.33 (abde)	8.13 (abde)	8.36 (abde)	6.53 (abe)
	$\beta_1$	1.46 (abde)	1.52 (ade)	1.38 (ade)	1.66 (abde)	1.61 (abde)	1.84 (abe)	1.28 (abe)
<b>Hummingbird</b>	$A_1$	7.09 (abe)	7.58 (abce)	7.64 (abce)	7.10 (abce)	7.21 (abce)	6.47 (abce)	-----
	$\beta_1$	1.71 (abce)	1.90 (abce)	1.98 (bce)	2.06 (bce)	2.00 (bce)	2.01 (b)	-----
<b>Cascade LX</b>	$A_1$	11.04 (abcd)	12.27 (abcd)	13.31 (abcd)	12.96 (abcd)	13.74 (abcd)	14.95 (abcd)	12.28 (abc)
	$\beta_1$	2.48 (abcd)	2.34 (abcd)	2.21 (abcd)	2.63 (abcd)	2.37 (abcd)	2.19 (abc)	2.43 (abc)

Table 4.2.  
Effect Size  $\Pi_1$  compared from each device to the bare head. Largest effect size greater than 1 highlighted.

	Schutt Stallion 650	Cascade CPX-R	Hummingbird	Cascade LX
Forehead	6.14	6.69	5.74	3.55
Forehead Oblique	7.77	6.22	4.29	3.34
Front Boss	6.75	6.14	4.04	2.43
Side	5.00	3.16	3.10	1.83
Rear Boss	4.91	3.94	3.80	1.92
RB-Obl	5.78	5.11	6.27	2.26
Rear	5.57	5.64	-----	3.07

Relative to the unhelmeted Hybrid III, the use of male lacrosse helmets consistently produced statistically significant reduction in the 2 values for the dimensionless angular accelerations for each helmet-location combination (Table 4.3). Female lacrosse helmets did not consistently produce statistically significant reductions for the dimensionless angular acceleration, with the Hummingbird failing to reduce the angular parameter between the Rear Boss, Rear Boss Oblique or Rear locations, and the Cascade LX failing to reduce the angular parameter significantly at the Front Boss or Rear Boss Oblique locations. The Cascade LX exhibited significantly lower A2 values than the Hummingbird, and male helmets at the Front. The Hummingbird helmets had significantly lower A2 values at the Front Oblique, and Front Boss locations than did the Schutt Stallion, Cascade CPX-R or Cascade LX.

Table 4.3.

Parameter values in for A and  $\beta_2$  in each cell with results from ANCOVA for the dimensionless translational acceleration parameter,  $\Pi_2$  between types of headgear denoted with letters. The annotations, a, b, c, d, and e indicate significant difference ( $p < 0.05$ ) between the regression parameters of the unhelmeted Hybrid III, Schutt Stallion 650, Cascade CPX-R, Hummingbird and Cascade LX respectively.

Locations								
		1	2	3	4	5	6	7
<b>Hybrid III</b>	$A_2$	6.05 (bcde)	10.65 (bcde)	10.16 (bcde)	14.82 (bcde)	10.69 (bcde)	7.43 (bcde)	4.22 (bc)
	$\beta_2$	1.73 (bcde)	2.09 (bcde)	1.77 (bcd)	2.10 (bcde)	2.00 (bce)	1.99 (bc)	1.56 (bce)
<b>Schutt Stallion 650</b>	$A_2$	5.43 (acde)	5.60 (acde)	5.41 (acde)	4.89 (ace)	3.47 (acde)	2.69 (acde)	3.05 (ae)
	$\beta_2$	1.25 (a)	1.09 (ade)	1.45 (ae)	0.87 (acde)	1.06 (acde)	0.78 (acde)	0.99 (ae)
<b>Cascade CPX-R</b>	$A_2$	5.51 (abde)	5.23 (abde)	4.17 (abde)	5.19 (abde)	5.07 (abde)	5.50 (abde)	3.11 (ae)
	$\beta_2$	1.23 (ad)	1.13 (ade)	1.32 (ae)	1.62 (abe)	1.47 (abde)	1.72 (abe)	0.96 (ae)
<b>Hummingbird</b>	$A_2$	3.94 (abce)	3.27 (abce)	3.33 (abce)	4.75 (ace)	5.93 (abce)	4.54 (abce)	-----
	$\beta_2$	1.38 (ac)	1.37 (abc)	1.43 (ae)	1.45 (abe)	1.91 (bce)	1.76 (be)	-----
<b>Cascade LX</b>	$A_2$	2.68 (abcd)	3.66 (abcd)	7.33 (abcd)	9.95 (abcd)	7.22 (abcd)	7.04 (abcd)	4.11 (bc)
	$\beta_2$	1.33 (a)	1.47 (abc)	1.91 (bcd)	2.24 (abcd)	2.31 (abcd)	2.13 (bcd)	1.72 (abc)

The effect size values for the dimensionless angular acceleration were significantly more variable between devices (Table 4.4). More than half of the values (18/28) were greater than unity when compared to the bare headform, with the Cascade LX demonstrating the most substantial effect size at the front location, the Hummingbird demonstrating the most substantial effect size at the Front Oblique and Front Boss

locations, and the Schutt Stallion 650 providing the most substantial effect size at the rest of the tested locations.

Table 4.4.  
Effect Size  $\Pi_2$  compared from each device to the bare head. Largest effect size greater than 1 highlighted.

	Schutt Stallion 650	Cascade CPX-R	Hummingbird	Cascade LX
Forehead	0.60	0.47	0.94	1.73
Forehead Oblique	3.00	2.85	4.11	3.62
Front Boss	1.50	2.09	2.68	0.89
Side	4.18	3.09	3.16	1.87
Rear Boss	3.14	1.86	1.86	1.24
RB-Obl	2.13	0.73	0.91	0.10
Rear	0.90	0.75	-----	0.10

Additionally, plots for each impact location were generated for the non-dimensional parameters for visual comparison (Figures 4.1, 4.2).

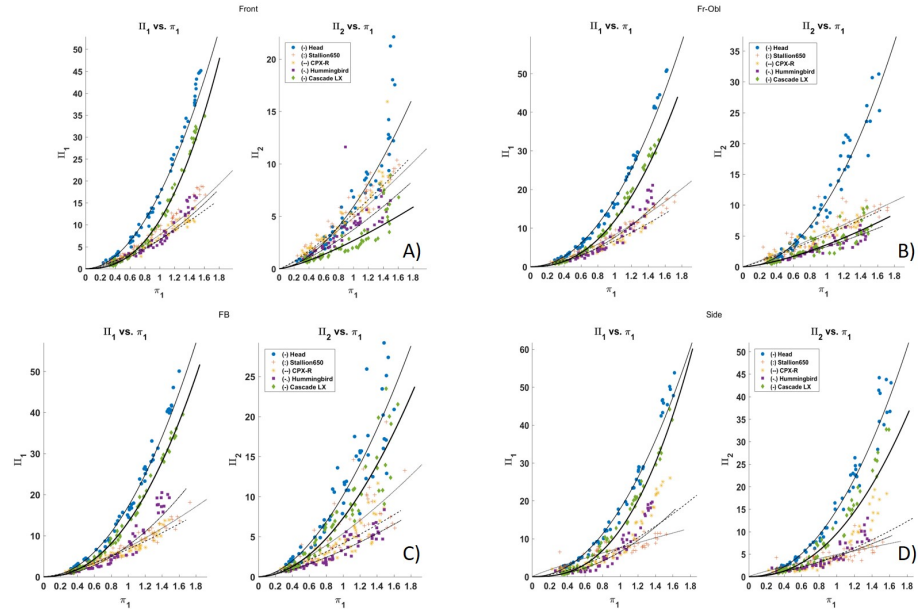


Figure 4.1. Front, Front-Oblique, Front Boss, and Side impact location data appear in A-D respectively

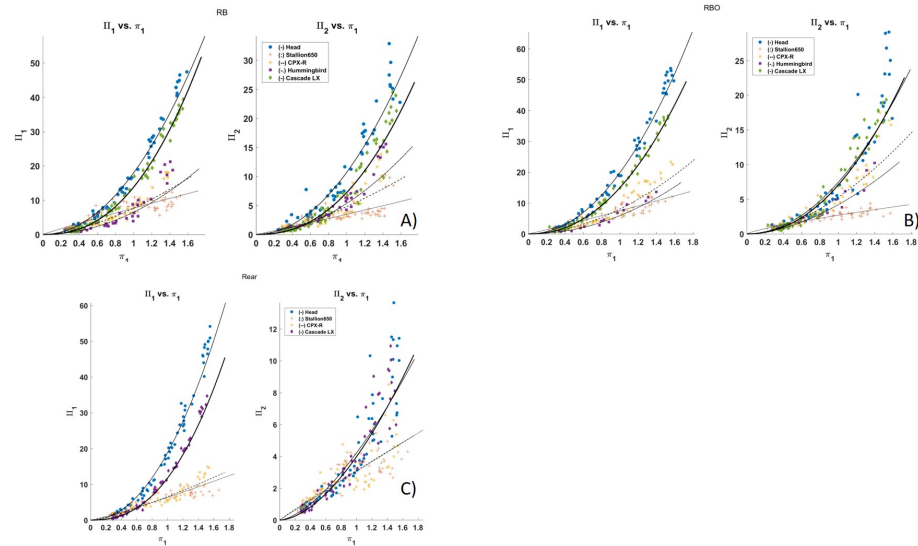


Figure 4.2. Rear Boss, Rear Boss Oblique, and Rear impact location data appear in A-C respectively.

Photos of the helmets were taken after the impacts were delivered (Figure 4.3.



Figure 4.3. Photos of the four helmets tested, from top to bottom and left to right, the Cascade LX, Hummingbird, Cascade CPXR, and Schutt Stallion 650.

#### 4.5 Discussion

The goal of this study was to quantify the impulse delivered to the headform-helmet system and the resultant translational and angular accelerations to provide a transfer function as previously proscribed by Cummiskey et. al to assess the performance of male and female lacrosse helmets. An intermediate asymptotic relationship was utilized to provide curve fitting parameters and generate statistical comparisons [37].

We found that the ability of male and female lacrosse helmets to attenuate the impacts delivered varied by the device and location. There was a clear effect of the

mass added by the helmet, type of padding, and in the case of the Hummingbird helmet, damage accumulation. For translational acceleration, the male lacrosse helmets consistently (7 of 7 locations) provided the best performance. The results were more varied for angular accelerations, but the Schutt performed best at 4 of the 7 locations again.

The effect size data indicated that the Cascade CPXR and the Schutt Stallion helmet possess design features that allow them to attenuate translational acceleration more effectively than the other helmet designs. This may be due to the mass of the helmets being higher than the female lacrosse helmets. It may also be accounted for due to the hard outer shells flexing during impact and dissipating some energy.

The effect size data indicated that the Cascade LX and Hummingbird possess design features that allow them to attenuate significant amounts of angular acceleration despite their performance being less desirable with respect to translational acceleration. The Cascade LX has a flexible polymer outer shell that may contribute to the better attenuation clearly visible at the first two locations, however this design seems to fair less well at other tested locations. The Hummingbird performed better with respect to translational acceleration than the Cascade LX and beat all of the tested helmets at attenuating angular acceleration at the Front Oblique and Front Boss location (Figure 4.1B and 4.1C). The Hummingbird may have suffered plastic deformation through the testing process, as the button that holds two pieces of the helmet together failed prior to the end of testing for all three of the tested devices.

Previous research focused on the use of the NOCSAE drop test as the primary mode of testing. It was used to demonstrate that football helmets dramatically outperform lacrosse helmets in the laboratory however no previous research has compared male and female lacrosse helmets [49]. Given that head accelerations are similar in football, womens soccer, and mens and womens lacrosse (Citations), considerable design improvements should be incorporated into lacrosse helmets especially those worn in womens lacrosse.

## 5. YOUTH VS. ADULT FOOTBALL HELMETS

*Material found in this chapter has or will appear in a journal publication*

### 5.1 Abstract

A large percentage of football athletes, as well as those who participate in other contact and collision sports show substantial negative changes in neurocognitive function, even over the course of a single season, motivating a need for improved safety systems. Previous studies have examined football helmets, and one study has compared youth and adult helmets and found no significant difference in performance. This study quantifies the transfer function connecting inputs and outputs of the system to provide a comparison of the impact attenuation capability youth and adult football helmets to reduce acceleration on the Hybrid III headform. Of those helmets tested, no significant difference between youth and adult models was found, as in prior studies. Future studies should utilize these data as a reference to inform future design for youth-specific helmet design focused on mitigating the range of impacts more commonly seen in youth football rather than those in high school and higher-level football. Future work should also develop better experimental modeling focused on the lower impact forces seen in middle school attenuation with a more compliant neck model than the Hybrid III 50th Percentile male headform to better simulate youth head impacts.

### 5.2 Introduction

Physiological changes resulting from repetitive head impacts in athletes are well documented [13,14,17–21]. Middle school players experience similar head acceleration events to their high school counterparts [52,53]. Youth players are nominally defined

as less than 14 years of age and no common restriction on helmet type by age group exists [54]. Middle school players experience the same acceleration, however no on-field data exists measuring the forces involved in the impacts sustained by each level of player.

Current test standards for youth and adult football helmets for play in football involve both drop tower and hydraulic ram tests, however both of those tests are specified with velocity input constraints [36]. These standards still do not yield an input-output relationship between impact force and resultant acceleration. Testing for both helmet styles is performed on modified small, medium, and large NOCSAE headforms utilizing a Hybrid III 50th percentile male headform. Youth helmets are tested at a lower velocity than the adult helmets and differ from adult models [36]. Prior testing has found that youth and adult helmets have nearly the same performance characteristics, excepting for a small difference in mass between youth and adult helmets of the same model due to the that they have ABS shells rather than polycarbonate shells [54]. The overall goal of this study was to evaluate the ability of youth and adult helmets to attenuate acceleration using a common, modal hammer-based protocol that quantifies the input load and output accelerations.

### 5.3 Methods

The study was designed to test the effectiveness of two size large helmet models designed for football in both the youth and adult models from Xenith (Xenith; Detroit, MI) , the Xenith Epic+ Youth and Xenith Epic+ Adult, as well as two from Riddell (Riddell; Rosemont, IL), the SpeedFlex Youth and the SpeedFlex adult. The mass of each helmet was measured three times and averaged to minimize error. The Xenith Epic+ Youth had a mass of 1.95kg the Xenith Epic+ Adult had a mass of 2.00kg the Riddell SpeedFlex Youth had a mass of 1.93 kg SpeedFlex Adult had a mass of 2.07kg. Each helmet was fitted to a 50th percentile Hybrid III headform testing rig, secured to a steel baseplate. Subsequently, the helmet was struck repeatedly at 10

different locations. The 20 impacts at each location were equally divided into five distinct impulse ranges from 2-4Ns, 5-7Ns, 8-10Ns, 11-13Ns, 14+Ns. Each headgear model was tested in triplicate for a total of 600 data points collected per protective device to correct for any qualities that may be the result of a defect in a single device. During testing, fracture lines were noticeable in the Youth Helmets that may have affected results on the second round of frontal impacts. The testing was post-processed utilizing the same methodology previously described in the background chapter.

## 5.4 Results

Relative to the unhelmeted Hybrid III each helmet significantly reduced dimensional translational and angular acceleration exponential components at each location, with the exception of the Speed Flex adult at the FR2-Oblique location testing the Flap on the Speed Flex helmets (Table 5.1 and Table 5.2). Additionally, the graphs for the output non-dimensional parameters can be seen in (Figures 5.1, 5.2, 5.3).

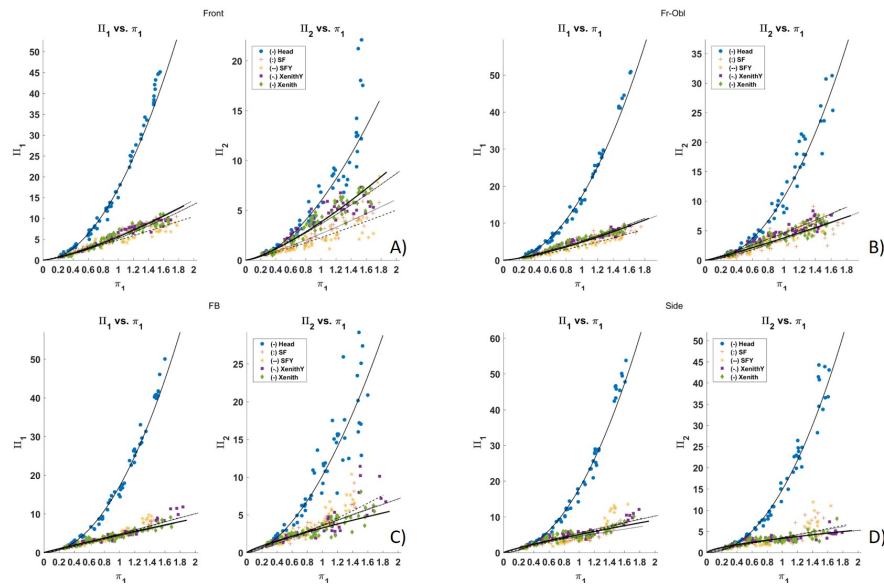


Figure 5.1. Front, Front-Oblique, Front Boss, and Side impact location data appear in A-D respectively

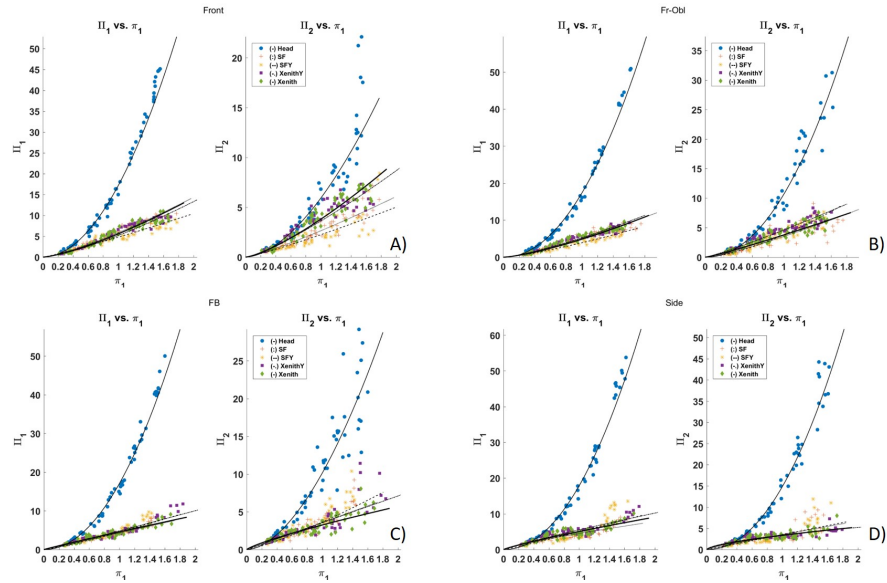


Figure 5.2. Rear Boss, Rear Boss Oblique, Rear, and Top impact location data appear in A-C respectively. impact location data appear in A-D respectively

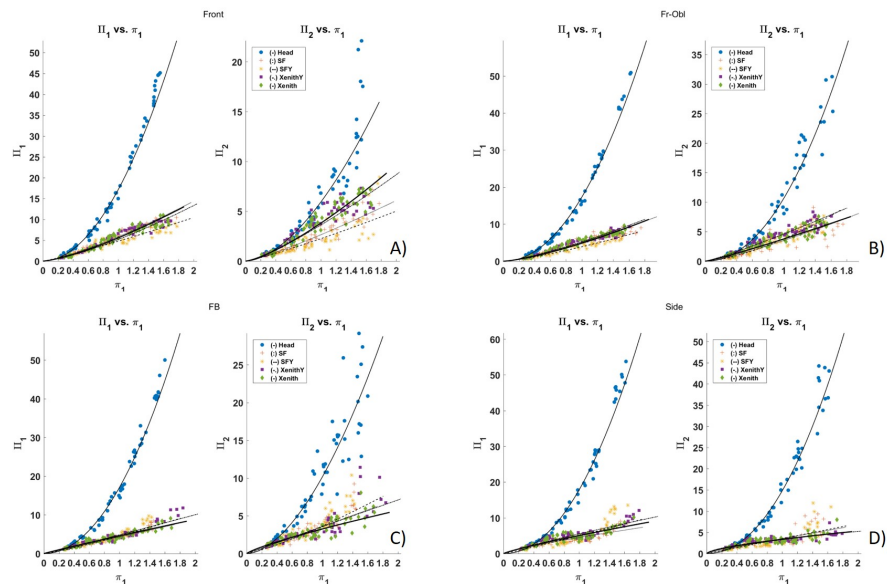


Figure 5.3. Front, Front-Oblique, Front Boss, and Side impact location data appear in A-D respectively

Table 5.1.

Parameter values in for  $A$  and  $\beta$  in each cell with results from ANCOVA for the dimensionless translational acceleration parameter,  $\Pi_1$  between types of headgear denoted with letters. The annotations, a, b, c, d, and e indicate significant difference between unhelmeted Hybrid III, Riddell Speed Flex, Riddell Speed Flex Youth, Xenith Epic+ Youth and Xenith Epic+ respectively.

		Locations								
		Front	Front-O	Front Boss	Side	Rear Boss	Rear Boss-O	Rear	Fr2	Fr2-Obl
<b>Hybrid III</b>	$A_1$	17.54 (bcde)	17.31 (bcde)	17.14 (bcde)	17.87 (bcde)	17.92 (bcde)	19.81 (bcde)	18.85 (bcde)	15.48 (bcde)	15.79 (bcde)
	$\beta_1$	1.96 (bcde)	2.06 (bcde)	2.04 (bcde)	2.07 (bcde)	2.02 (bcde)	2.05 (bcde)	2.08 (bcde)	2.16 (bcde)	2.20 (bcde)
<b>Riddell Speed Flex</b>	$A_1$	5.86 (acde)	5.09 (acde)	4.52 (acde)	4.50 (acde)	4.68 (ade)	4.41 (acde)	5.67 (ade)	4.35 (acde)	4.84 (acde)
	$\beta_1$	1.29 (ac)	1.28 (a)	1.02 (ac)	0.80 (ac)	0.96 (a)	0.94 (ac)	1.04 (ac)	1.26 (acde)	1.39 (acde)
<b>Riddell Speed Flex Youth</b>	$A_1$	4.79 (abde)	3.90 (abde)	5.14 (abde)	5.01 (abd)	4.55 (ade)	5.47 (abd)	5.65 (ade)	3.57 (abde)	4.36 (abde)
	$\beta_1$	1.12 (abde)	1.30 (a)	1.19 (abde)	1.07 (abde)	1.06 (ae)	1.39 (abde)	0.85 (abde)	0.98 (abde)	1.32 (abde)
<b>Xenith Epic+ Youth</b>	$A_1$	5.75 (abce)	5.24 (abc)	4.86 (abce)	5.64 (abce)	6.63 (abce)	5.95 (abce)	7.52 (abc)	5.55 (abce)	4.74 (abce)
	$\beta_1$	1.36 (ac)	1.31 (a)	1.05 (ace)	0.89 (ac)	0.94 (a)	0.95 (ac)	0.99 (ac)	1.48 (abc)	1.12 (abce)
<b>Xenith Epic+</b>	$A_1$	5.58 (abcd)	5.25 (abc)	4.59 (abcd)	5.05 (abd)	5.97 (abcd)	5.26 (abd)	7.37 (abc)	5.16 (abcd)	5.11 (abcd)
	$\beta_1$	1.35 (ac)	1.37 (a)	0.95 (acd)	0.85 (ac)	0.88 (ac)	0.89 (ac)	1.04 (ac)	1.44 (abc)	1.22 (abcd)

Table 5.2.

Parameter values in for  $A$  and  $\beta$  in each cell with results from ANCOVA for the dimensionless translational acceleration parameter,  $\Pi_2$  between types of headgear denoted with letters. The annotations, a, b, c, d, and e indicate significant difference between unhelmeted Hybrid III, Riddell Speed Flex, Riddell Speed Flex Youth, Xenith Epic+ Youth and Xenith Epic+ respectively.

Locations										
		Front	Front-O	Front Boss	Side	Rear Boss	Rear Boss-O	Rear	Fr2	Fr2-Obl
<b>Hybrid III</b>	$A_1$	6.05 (bcde)	10.65 (bcde)	10.16 (bcde)	14.82 (bcde)	10.69 (bcde)	7.43 (bcde)	4.22 (bcde)	5.09 (bce)	4.36 (bcde)
	$\beta_1$	1.73 (bcde)	2.09 (bcde)	1.77 (bcde)	2.10 (bcde)	2.00 (bcde)	1.99 (bcde)	1.56 (bcde)	2.08 (bcde)	1.52 (cde)
<b>Riddell Speed Flex</b>	$A_1$	2.65 (acde)	3.50 (acde)	3.78 (acde)	3.54 (ae)	2.80 (ade)	2.58 (acde)	2.06 (acde)	2.20 (acde)	2.60 (acde)
	$\beta_1$	1.20 (ae)	1.25 (ac)	1.01 (ace)	0.92 (ade)	0.96 (a)	0.91 (ac)	1.08 (a)	0.97 (a)	1.46 (cde)
<b>Riddell Speed Flex Youth</b>	$A_1$	2.26 (abde)	3.79 (abde)	4.16 (abde)	3.53 (ae)	2.82 (ade)	4.26 (abd)	2.00 (abde)	2.07 (abde)	1.79 (abde)
	$\beta_1$	1.15 (ae)	1.51 (abde)	1.24 (abde)	1.01 (ade)	1.03 (ae)	1.35 (abde)	0.95 (ade)	0.94 (a)	1.21 (abde)
<b>Xenith Epic+ Youth</b>	$A_1$	3.98 (abce)	4.61 (abce)	3.57 (abce)	3.47 (ae)	4.84 (abce)	5.73 (abce)	2.93 (abce)	5.21 (bce)	3.21 (abce)
	$\beta_1$	1.26 (a)	1.13 (ac)	0.99 (ace)	0.61 (abc)	0.93 (a)	1.00 (ac)	1.07 (ac)	1.04 (a)	0.98 (abc)
<b>Xenith Epic+</b>	$A_1$	3.81 (abcd)	4.02 (abcd)	3.26 (abcd)	3.35 (abcd)	4.16 (abcd)	4.48 (abd)	3.34 (abcd)	4.74 (abcd)	3.74 (abcd)
	$\beta_1$	1.34 (abc)	1.13 (ac)	0.81 (abcd)	0.67 (abc)	0.85 (ac)	0.87 (ac)	1.10 (ac)	1.06 (a)	1.00 (abc)

At that location the coefficient parameter was still significantly different from the H3H. All helmets tested provided substantial effect sizes when compared to the bare head at all locations for both  $P_{i_1}$  and  $P_{i_2}$ , and thus were omitted from results.

When comparing effect size between helmets of the same brand to determine a difference between Youth and Adult models of the same helmet it was found that the

Speed Flex Youth helmet was substantially different than the Adult helmet at the Front, Front Oblique, and FR2-Oblique test locations for the  $\Pi_1$  parameter (Table 5.3).

Table 5.3.

Effect size measures between each pair of helmets for the dimensionless translational acceleration,  $\Pi_1$ . Highlights occur where a helmet is substantially different between the youth and adult versions.

Locations										
		Front	Front-O	Front Boss	Side	Rear Boss	Rear Boss-O	Rear	Fr2	Fr2-Obl
<b>Hybrid III</b>	$A_1$	6.05 (bcde)	10.65 (bcde)	10.16 (bcde)	14.82 (bcde)	10.69 (bcde)	7.43 (bcde)	4.22 (bcde)	5.09 (bce)	4.36 (bcde)
	$\beta_1$	1.73 (bcde)	2.09 (bcde)	1.77 (bcde)	2.10 (bcde)	2.00 (bcde)	1.99 (bcde)	1.56 (bcde)	2.08 (bcde)	1.52 (cde)
<b>Riddell Speed Flex</b>	$A_1$	2.65 (acde)	3.50 (acde)	3.78 (acde)	3.54 (ae)	2.80 (ade)	2.58 (acde)	2.06 (acde)	2.20 (acde)	2.60 (acde)
	$\beta_1$	1.20 (ae)	1.25 (ac)	1.01 (ace)	0.92 (ade)	0.96 (a)	0.91 (ac)	1.08 (a)	0.97 (a)	1.46 (cde)
<b>Riddell Speed Flex Youth</b>	$A_1$	2.26 (abde)	3.79 (abde)	4.16 (abde)	3.53 (ae)	2.82 (ade)	4.26 (abd)	2.00 (abde)	2.07 (abde)	1.79 (abde)
	$\beta_1$	1.15 (ae)	1.51 (abde)	1.24 (abde)	1.01 (ade)	1.03 (ae)	1.35 (abde)	0.95 (ade)	0.94 (a)	1.21 (abde)
<b>Xenith Epic+ Youth</b>	$A_1$	3.98 (abce)	4.61 (abce)	3.57 (abce)	3.47 (ae)	4.84 (abce)	5.73 (abce)	2.93 (abce)	5.21 (bce)	3.21 (abce)
	$\beta_1$	1.26 (a)	1.13 (ac)	0.99 (ace)	0.61 (abc)	0.93 (a)	1.00 (ac)	1.07 (ac)	1.04 (a)	0.98 (abc)
<b>Xenith Epic+</b>	$A_1$	3.81 (abcd)	4.02 (abcd)	3.26 (abcd)	3.35 (abcd)	4.16 (abcd)	4.48 (abd)	3.34 (abcd)	4.74 (abcd)	3.74 (abcd)
	$\beta_1$	1.34 (abc)	1.13 (ac)	0.81 (abcd)	0.67 (abc)	0.85 (ac)	0.87 (ac)	1.10 (ac)	1.06 (a)	1.00 (abc)

In these cases, from the graphs the Speed Flex Youth was producing lower translational and angular acceleration than the Speed Flex adult (Figure 5.1A, 5.1B). It should be noted however that the Speed Flex Youth helmet displayed significant

damage during the course of testing, with cracks forming during the Front Oblique testing and lengthening throughout the testing procedure (Figure 5.4). The Xenith Epic+ Youth helmet was not substantially different from the Xenith Epic+ Adult helmet at any location with respect to the effect size calculation for the translational parameter (Table 5.3).



Figure 5.4. Crack length visible on various helmets. A) is the Riddell Youth Speed Flex, B) and C) are the Xenith Epic+ Youth, D) is the Riddell Speed Flex, E) and F) are the Xenith Epic+ helmets.

The effect size differences between the Speed Flex Youth and Speed Flex Adult helmets were insubstantial at all locations tested with respect to the  $Pi_2$  dimensionless angular acceleration parameter (Table 5.4).

Table 5.4.

Effect size measures between each pair of helmets for the dimensionless angular acceleration,  $\Pi_2$ . Highlights occur where a helmet is substantially different between the youth and adult versions.

		Locations								
		Front	Front-O	Front Boss	Side	Rear Boss	Rear Boss-O	Rear	Fr2	Fr2-Obl
<b>Hybrid III</b>	$A_1$	6.05 (bcde)	10.65 (bcde)	10.16 (bcde)	14.82 (bcde)	10.69 (bcde)	7.43 (bcde)	4.22 (bcde)	5.09 (bce)	4.36 (bcde)
	$\beta_1$	1.73 (bcde)	2.09 (bcde)	1.77 (bcde)	2.10 (bcde)	2.00 (bcde)	1.99 (bcde)	1.56 (bcde)	2.08 (bcde)	1.52 (cde)
<b>Riddell Speed Flex</b>	$A_1$	2.65 (acde)	3.50 (acde)	3.78 (acde)	3.54 (ae)	2.80 (ade)	2.58 (acde)	2.06 (acde)	2.20 (acde)	2.60 (acde)
	$\beta_1$	1.20 (ae)	1.25 (ac)	1.01 (ace)	0.92 (ade)	0.96 (a)	0.91 (ac)	1.08 (a)	0.97 (a)	1.46 (cde)
<b>Riddell Speed Flex Youth</b>	$A_1$	2.26 (abde)	3.79 (abde)	4.16 (abde)	3.53 (ae)	2.82 (ade)	4.26 (abd)	2.00 (abde)	2.07 (abde)	1.79 (abde)
	$\beta_1$	1.15 (ae)	1.51 (abde)	1.24 (abde)	1.01 (ade)	1.03 (ae)	1.35 (abde)	0.95 (ade)	0.94 (a)	1.21 (abde)
<b>Xenith Epic+ Youth</b>	$A_1$	3.98 (abce)	4.61 (abce)	3.57 (abce)	3.47 (ae)	4.84 (abce)	5.73 (abce)	2.93 (abce)	5.21 (bce)	3.21 (abce)
	$\beta_1$	1.26 (a)	1.13 (ac)	0.99 (ace)	0.61 (abc)	0.93 (a)	1.00 (ac)	1.07 (ac)	1.04 (a)	0.98 (abc)
<b>Xenith Epic+</b>	$A_1$	3.81 (abcd)	4.02 (abcd)	3.26 (abcd)	3.35 (abcd)	4.16 (abcd)	4.48 (abd)	3.34 (abcd)	4.74 (abcd)	3.74 (abcd)
	$\beta_1$	1.34 (abc)	1.13 (ac)	0.81 (abcd)	0.67 (abc)	0.85 (ac)	0.87 (ac)	1.10 (ac)	1.06 (a)	1.00 (abc)

The Xenith Epic+ Youth helmet was substantially different than the Xenith Epic+ Adult helmet at the FR2-Oblique test location and produced substantially lower angular acceleration than the Adult helmet of the same model.

## 5.5 Discussion

The goal of this study was to quantify the impulse delivered to the headform-helmet system and the resultant translational and angular acceleration to provide a transfer function as previously proscribed by Cummiskey et al. to assess the performance of youth and adult football helmets. An intermediate asymptotic relationship was utilized to provide curve fitting parameters and generate statistical comparisons [37].

We found that the ability of youth and adult helmets to attenuate the impacts delivered varied by device and location. The Adult helmets showed only light wear and tear from the testing protocol, whereas the Youth helmets of Riddell showing significantly more wear, with large cracks, with the largest more than 2 inches in length compared to the Xenith helmets which have similar wear (Figure 5.4). For translational acceleration the Youth SpeedFlex helmet outperformed the Adult SpeedFlex however this may have been due to the crack formation from the ABS shell of the Youth SpeedFlex. The Xenith Epic+ Youth and Adult shells experienced similar amounts of crack propagation in the same regions, indicating that the crack damage may be the result of the shape of the slits in the helmet shell rather than the material the shell is made from.

For the majority of locations, the helmets had no substantial difference in performance between the Youth and Adult helmets according to the effect size calculations except for their resilience to damage. One interesting performance characteristic is the shape of the impact response curves for the Side impact location, which have a very similar appearance to stress-strain curves for foam materials. This may indicate that the padding on the side has entered a condensing phase, meaning that it is no longer removing energy from the system.

NOCSAE currently does not separately mandate standards for Youth and Adult helmets, rather, they certify the Youth helmets at lower impact velocities than Adult helmets and place no restrictions on which age group can wear the NOCSAE cer-

tified Youth Helmets. Previous research has corroborated the lack of performance differences between Youth and Adult helmets of the same model. Interestingly, this indicates that the Youth helmets were not designed with the forces typically experienced at the level of play Youth helmets are intended to be worn in mind. Given that head accelerations are similar in middle school, and high school football, but the forces are not, future research should identify the range of forces in youth football impacts, as well as modeling youth impacts experimentally for new helmet certification with a more compliant neck structure than the Hybrid III 50th Percentile male neck.

With knowledge of the forces typically experienced, padding can be tailored to absorb more energy from the lower force impacts, rather than the stiffer padding that performs better for higher force impacts and prevent padding from entering the condensing phase at too low of a stress. Current helmet designs are fundamentally limited with respect to the performance they can achieve because they are missing the force data, which the current NOCSAE standard most helmets are tailored to pass does not include or consider. With a better Youth head and neck model, new helmets can be tailored to attenuate the maximum energy for each level of play. Ultimately, this could lead to the development of position specific headgear as well if specific trends can be identified in players by level of play in the NCAA, NFL, and XFL. Future work should also investigate how helmet performance has evolved in the last ten years since concussion and traumatic brain injury gained national attention.

## **5.6 Acknowledgments**

Xenith provided the helmets tested in this chapter.

## 6. 2018 FOOTBALL HELMET ROUNDUP

*Material found in this chapter has or will appear in a journal publication.*

*At this time the data for 2 helmets have yet to be collected.*

### 6.1 Abstract

Significant numbers of athletes playing football, and those who participate in other contact and collision sports show substantial negative changes in neurocognitive function, even over the course of a single season. This has motivated research into new technologies that improve helmet performance. Prior studies have examined football helmets, and performance metrics in detail, however no paper has compared improvements to various brand helmet performance over time and quantified the performance of helmets and brands that did not exist at the time of the first study of this kind. This study quantifies the transfer function connecting inputs and outputs of the system to provide a comparison of the impact attenuation of various adult football helmets to reduce acceleration on the Hybrid III headform. Of those helmets tested, design features were compared with performance metrics to determine desirable features. Future studies should utilize these data as a reference to inform future design for helmet design focused on mitigating the range of impacts more commonly seen in football as well as those seen by level of play. Future work should investigate the performance of helmets tailored by level of play.

### 6.2 Introduction

How has helmet performance evolved since 2013 when the group began testing football helmets with this methodology.

### 6.3 Methods

The study was designed to test the effectiveness of several size large helmet models designed for football in adult models from Xenith (Xenith; Detroit, MI) , the Xenith Epic+ and X2E+, as well as three from Riddell (Riddell; Rosemont, IL), the Speed Flex, the Speed Icon, and the Speed, one helmet from Vicis (Seattle; WA) the Zero 1 and three helmets from Schutt (Litchfield, IL), the Air XP Pro VTD II, the Vengeance VTD II and the Vengeance Pro. The mass of each helmet was measured three times and averaged to minimize error. The mass of each helmet was measured three times and averaged to minimize error. The Schutt Air XP Pro VTD II had a mass of 2.018kg, the Vengeance VTD II 1.94kg, the Vengeance Pro 1.72kg, Xenith X2E+ 1.942kg, Xenith Epic+ 1.96kg, the Speed Flex 2.02kg, the Speed Icon 1.825kg, the Speed Classic 1.813kg, Vicis Zero 1 2.103kg.

Each helmet was fitted to a 50th percentile Hybrid III headform testing rig, secured to a steel baseplate. Subsequently, the helmet was struck repeatedly at 14 different locations. The 20 impacts at each location were equally divided into five distinct impulse ranges from 2-4Ns, 5-7Ns, 8-10Ns, 11-13Ns, 14+Ns. Each headgear model was tested in triplicate for a total of 840 data points collected per protective device to correct for any qualities that may be the result of a defect in a single device. The testing was post-processed utilizing the same methodology previously described in the background chapter.

### 6.4 Results

For each helmet tested, comparison graphs for the dimensionless parameters were generated (Figures 6.1, 6.2).

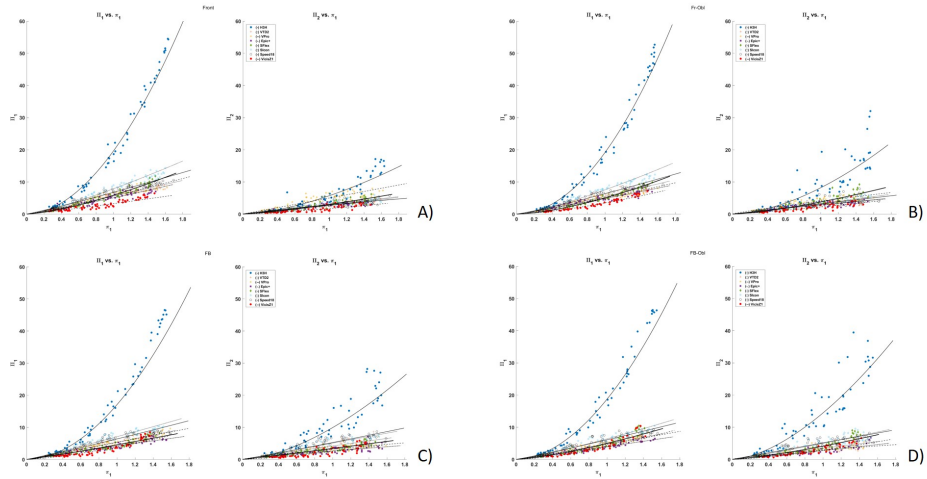


Figure 6.1. Front, Front-Oblique, Front Boss, and Front Boss-Oblique impact location data appear in A-D respectively for the 2018 football helmets.

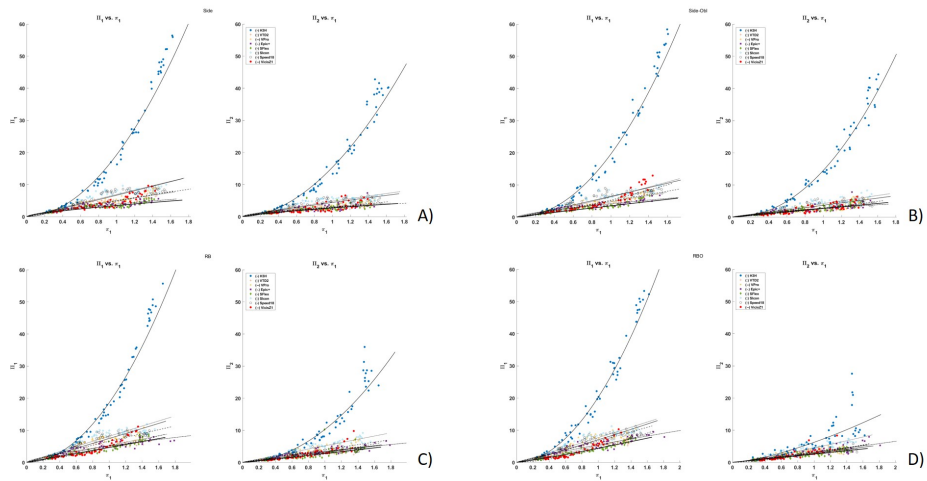


Figure 6.2. Side, Side-Oblique, Rear Boss, and Rear Boss-Oblique impact location data appear in A-D respectively for the 2018 football helmets.

The parameter values for each location were generated for the dimensionless translational and angular acceleration components were generated to establish significant differences between the equations describing each helmets behavior (Tables 6.1). Rel-

ative to the unhelmeted Hybrid III the helmets consistently provided statistically significant reductions in slope at each location.

Table 6.1.

Parameter values in for A and  $\beta_1$  in each cell with results from ANCOVA for the dimensionless translational acceleration parameter,  $\Pi_1$  between types of headgear denoted with letters. The annotations, a, b, c, d, e, f and g indicate significant difference ( $p < 0.05$ ) between the regression parameters of the unhelmeted Hybrid III, the Schutt Air XP Pro VTD II, the Vengeance VTD II, the Vengeance Pro, Xenith X2E+, Xenith Epic+, the Speed Flex, the Speed Icon, the Speed Classic, and the Vicis Zero 1.

		Locations								
		Front	F-Obl	Front Boss	Side	Rear Boss	RB - Obl	Rear	Fr2	Fr2-Obl
<b>Hybrid III</b>	$A_1$	19.57 (bcdefg)	19.08 (bcdefg)	18.32 (bcdefg)	19.26 (bcdefg)	18.53 (bcdefg)	20.21 (bcdefg)	20.14 (bcdefg)	15.90 (bcdefg)	19.01 (bcdefg)
	$\beta_1$	1.90 (bcdefg)	1.99 (bcdefg)	1.92 (bcdefg)	1.94 (bcdefg)	1.98 (bcdefg)	1.95 (bcdefg)	1.91 (bcdefg)	2.05 (bcdefg)	2.02 (bcdefg)
<b>Schutt Vengeance VTD II</b>	$A_1$	5.59 (acdefg)	5.49 (acdefg)	5.33 (adefg)	4.97 (acdefg)	5.26 (acdef)	5.33 (acdef)	5.41 (acdefg)	5.07 (acdefg)	4.86 (acdefg)
	$\beta_1$	1.06 (ace)	1.13 (aeg)	1.05 (ag)	0.87 (adefg)	0.97 (adg)	1.11 (adg)	1.08 (ag)	1.23 (aeg)	1.23 (acdeg)
<b>Schutt Vengeance Pro</b>	$A_1$	5.82 (abdfg)	5.04 (abdfg)	5.28 (adefg)	5.44 (abdefg)	7.07 (abdefg)	6.60 (abdefg)	7.79 (abdefg)	5.22 (abdefg)	4.54 (abdefg)
	$\beta_1$	1.16 (abe)	1.11 (aeg)	1.03 (ag)	0.90 (adefg)	0.93 (adg)	1.06 (adg)	1.04 (ag)	1.14 (aeg)	0.98 (abefg)
<b>Xenith Epic+</b>	$A_1$	5.04 (abcefg)	4.81 (abcefg)	4.17 (abcefg)	3.90 (abcefg)	5.10 (abcef)	5.43 (abcef)	6.81 (abceg)	4.38 (abcefg)	4.19 (abcefg)
	$\beta_1$	1.14 (ae)	1.10 (aeg)	0.96 (aefg)	0.67 (abcfg)	0.71 (abcefg)	0.86 (abcefg)	0.97 (ag)	1.17 (aeg)	1.08 (abefg)
<b>Riddell SpeedFlex 2018</b>	$A_1$	5.84 (abdfg)	5.01 (abdfg)	4.51 (abcdfg)	3.63 (abcdfg)	4.62 (abcdfg)	4.37 (abcdfg)	5.50 (abcdfg)	4.66 (abcdfg)	4.38 (abcdfg)
	$\beta_1$	1.43 (abcdfg)	1.54 (abcdfg)	1.12 (adg)	0.72 (abcfg)	1.00 (adg)	1.15 (adg)	1.03 (ag)	1.38 (abcdf)	1.42 (abcdfg)
<b>Riddell Speed</b>	$A_1$	6.75 (abcdeg)	6.32 (abcdeg)	6.34 (abcdeg)	6.67 (abcdeg)	7.43 (abcdeg)	6.99 (abcdeg)	6.91 (abceg)	5.87 (abcdeg)	5.64 (abcdeg)
	$\beta_1$	1.10 (ae)	1.15 (aeg)	1.09 (adg)	1.04 (abcde)	1.04 (adg)	1.13 (adg)	1.06 (ag)	1.14 (aeg)	1.21 (acdeg)
<b>Vicis Zero 1</b>	$A_1$	3.81 (abcd)	4.02 (abcd)	3.26 (abcd)	4.77 (abcdef)	5.09 (acef)	5.24 (acef)	5.16 (abcdef)	2.78 (abcdef)	2.99 (abcdef)
	$\beta_1$	1.34 (abc)	1.13 (ac)	0.81 (abcd)	1.04 (abcde)	1.23 (abcdef)	1.61 (abcdef)	1.37 (abcdef)	1.40 (abcdf)	1.61 (abcdef)

To better compare the helmets tested at each location an effect size measurement was utilized to establish whether substantial reductions in the given dimensionless parameters were experienced relative to the bare head (Tables 6.2 and 6.3).

Table 6.2.

Effect size measures between each helmet tested in the 2018 set relative to the bare head for the dimensionless translational acceleration,  $\Pi_1$ . Largest effect size greater than 1 highlighted.

	<b>Vengeance VTD II</b>	<b>Vengeance Pro</b>	<b>Epic +</b>	<b>Speed Flex</b>	<b>Speed Icon</b>	<b>Speed Classic</b>	<b>Zero 1</b>
<b>Forehead</b>	9.46	8.45	7.5	7.85	7.09	8.3	9.03
<b>F - Oblique</b>	7.16	7.97	7.67	8.49	6.3	7.09	8.52
<b>Front Boss</b>	6.76	7.7	8.43	7.1	5.99	6.26	6.08
<b>Side</b>	5.49	5.53	6.2	5.93	4.96	4.91	5.02
<b>Rear Boss</b>	5.97	4.1	7.47	6.11	4.46	4.23	4.38
<b>RB - Obl</b>	6.21	5.28	8.29	7.9	5.62	5.86	5.37
<b>Rear</b>	6.32	4.93	5.16	6.5	5.25	5.53	4.69
<b>Top</b>	6.36	5.48	5.15	5.97	4.24	5.31	5.8

For the dimensionless translational acceleration parameter, the Xenith Epic+ provided the largest substantial reduction at 4/8 locations, with the Schutt Vengeance VTD II accounting for 2/8, and the Riddell Speed Flex, and Vicis Zero 1 accounting for the final two.

Table 6.3.

Effect size measures between each helmet tested in the 2018 set relative to the bare head for the dimensionless angular acceleration,  $\Pi_2$ . Largest effect size greater than 1 highlighted.

	<b>Vengeance VTD II</b>	<b>Vengeance Pro</b>	<b>Epic +</b>	<b>Speed Flex</b>	<b>Speed Icon</b>	<b>Speed Classic</b>	<b>Zero 1</b>
<b>Forehead</b>	2.16	0.78	1.91	1.69	1.97	2.14	2.46
<b>F - Oblique</b>	1.82	1.51	1.88	1.41	1.8	1.63	1.94
<b>Front Boss</b>	2.14	2.89	3.16	2.73	1.97	1.9	2.55
<b>Side</b>	4.67	5.03	4.75	4.46	4.44	4.5	4.26
<b>Rear Boss</b>	3.17	2.18	3.73	2.72	2.37	2.94	2.19
<b>RB - Obl</b>	0.96	1.01	1.25	1.28	0.6	1.3	0.81
<b>Rear</b>	1.01	0.25	0.5	1.39	1.18	0.9	1.16
<b>Top</b>	0.91	0.72	0.47	0.83	0.65	0.75	0.84

For the dimensionless angular acceleration parameter, The Schutt Vengeance VTD II, Riddell Speed Flex, Riddell Speed Classic, and the Xenith Epic+ provided the largest substantial reduction at one location each, with the Schutt Vengeance Pro and Vicis Zero 1, accounting for two of the largest effect sizes each.

In addition to the comparison graphs for dimensionless parameters and effect size tables for the total set of helmets generated in 2018, comparisons to the original helmets tested in Cummiskey et al. were generated comparing the Riddell, Schutt, and Xenith helmets from 2014 and 2015 to those from 2018 [40]. The Riddell Speed Flex performed best at the majority of locations relative to the translational parameter (Figures 6.3 and Appendix B for extra figures removed from this chapter). The Speed Classic performs best at the majority of locations relative to the angular parameter.

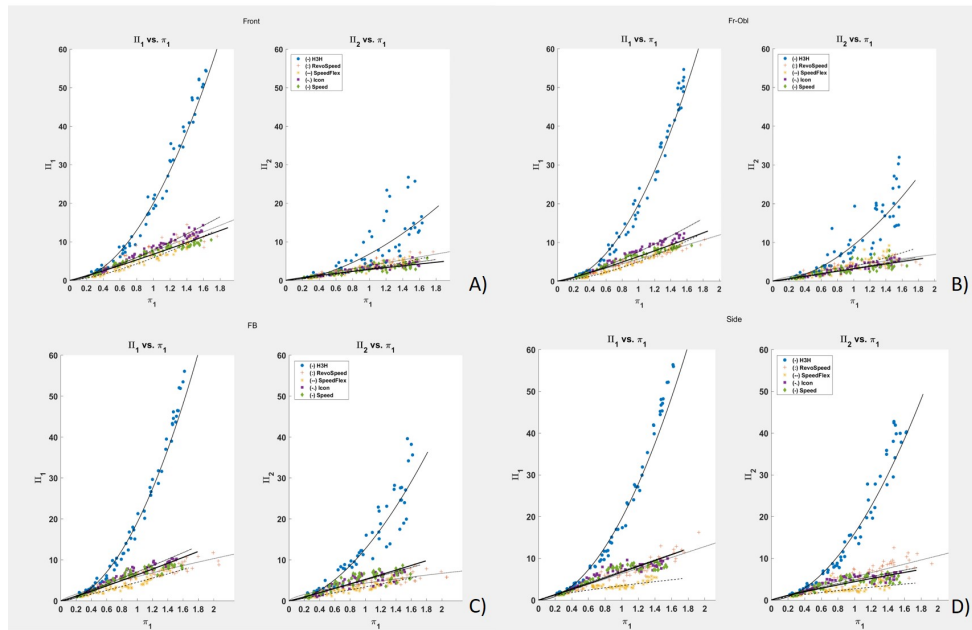


Figure 6.3. Front, Front-Oblique, Front Boss, and Side impact location data appear in A-D respectively for the Riddell helmets tested with this methodology.

Effect size calculations allow for more thorough examination of the performance of helmets (Tables 6.4 and 6.5). The Riddell Speed Flex has the largest effect size at 6/8 locations tested with respect to translational acceleration, and 1/8 locations for the angular parameter. The Riddell Speed Classic has the largest effect size at 5/8 locations relative to the angular parameter and 1/8 locations for the translational acceleration parameter.

Table 6.4.

Effect size measures between each Riddell helmet relative to the bare head for the dimensionless translational acceleration,  $\Pi_1$ . Largest effect size greater than 1 highlighted.

	<b>RevoSpeed</b>	<b>SpeedFlex</b>	<b>Speed Icon</b>	<b>Speed Classic</b>
<b>Forehead</b>	6.33	7.53	6.89	8.04
<b>F - Oblique</b>	7.75	8.85	6.63	7.42
<b>Front Boss</b>	7.8	7.26	6.22	6.91
<b>Side</b>	6.14	6.43	5.33	5.27
<b>Rear Boss</b>	4.94	6.21	4.62	4.36
<b>RB - Oblique</b>	5.38	7.09	5.11	5.34
<b>Rear</b>	6.41	7.92	6.1	5.95
<b>Top</b>	5.49	5.81	4.34	5.71

Table 6.5.

Effect size measures between each Riddell helmet relative to the bare head for the dimensionless angular acceleration,  $\Pi_2$ . Largest effect size greater than 1 highlighted.

	<b>RevoSpeed</b>	<b>SpeedFlex</b>	<b>Speed Icon</b>	<b>Speed Classic</b>
<b>Forehead</b>	1.17	1.2	1.37	1.49
<b>F - Oblique</b>	1.97	1.83	2.29	2.06
<b>Front Boss</b>	3.34	3.23	2.52	2.61
<b>Side</b>	4.13	4.54	4.55	4.61
<b>Rear Boss</b>	1.75	2.14	1.92	2.23
<b>RB - Oblique</b>	0.89	1.05	0.71	1.1
<b>Rear</b>	0.23	1.23	1.01	0.75
<b>Top</b>	1.24	2.04	1.63	2.08

The Schutt Vengeance VTD II provided the largest substantial reduction relative to the bare head at 6/8 locations tested with respect to the dimensionless translational parameter, and 3/8 locations with respect to the angular acceleration parameter. The Schutt Vengeance Pro provided the largest substantial reduction for 2/8 locations with respect to both the angular and translational parameters (Figures 6.4 and Appendix B).

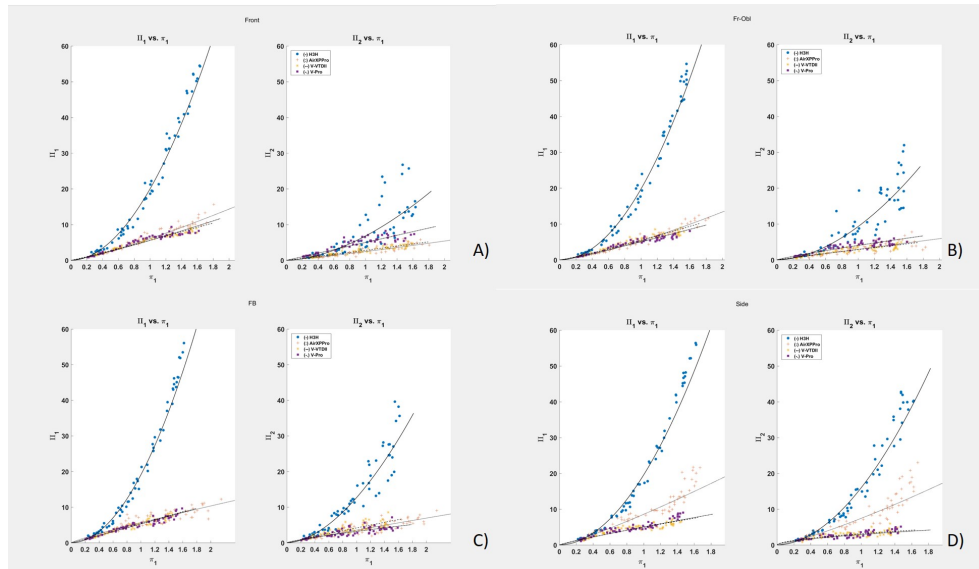


Figure 6.4. Front, Front-Oblique, Front Boss, and Side impact location data appear in A-D respectively for the Schutt helmets tested with this methodology.

The Schutt Vengeance VTD II provided the largest substantial reduction relative to the bare head at 6/8 locations tested with respect to the dimensionless translational parameter, and 3/8 locations with respect to the angular acceleration parameter (Tables 6.6 and 6.7). The Schutt Vengeance Pro provided the largest substantial reduction for 2/8 locations with respect to both the angular and translational parameters.

Table 6.6.

Effect size measures between each Schutt helmet relative to the bare head for the dimensionless translational acceleration,  $\Pi_1$ . Largest effect size greater than 1 highlighted.

	<b>Air XP Pro</b>	<b>Vengeance VTD II</b>	<b>Vengeance Pro</b>
<b>Forehead</b>	7.87	9.05	8.16
<b>F - Oblique</b>	7.89	7.47	8.31
<b>Front Boss</b>	7.01	6.92	8.4
<b>Side</b>	4.12	5.94	5.99
<b>Rear Boss</b>	4.51	6.08	4.22
<b>RB - Oblique</b>	3.22	5.57	4.79
<b>Rear</b>	5.78	7.82	5.76
<b>Top</b>	2.85	6.14	5.55

Table 6.7.

Effect size measures between each Schutt helmet relative to the bare head for the dimensionless angular acceleration,  $\Pi_2$ . Largest effect size greater than 1 highlighted.

	<b>Air XP Pro</b>	<b>Vengeance VTD II</b>	<b>Vengeance Pro</b>
<b>Forehead</b>	1.53	1.45	0.74
<b>F - Oblique</b>	2.18	2.29	1.97
<b>Front Boss</b>	3.38	2.62	3.61
<b>Side</b>	2.7	4.76	5.11
<b>Rear Boss</b>	1.15	2.37	1.72
<b>RB - Oblique</b>	0.49	0.85	0.91
<b>Rear</b>	0.52	0.88	0.23
<b>Top</b>	1.51	2.22	1.86

The Xenith helmets were very near in performance in translational and angular acceleration parameters at the front, front oblique, and front boss locations, with larger differences notable at the side, and rear boss locations (Figures 6.5 and Appendix B).

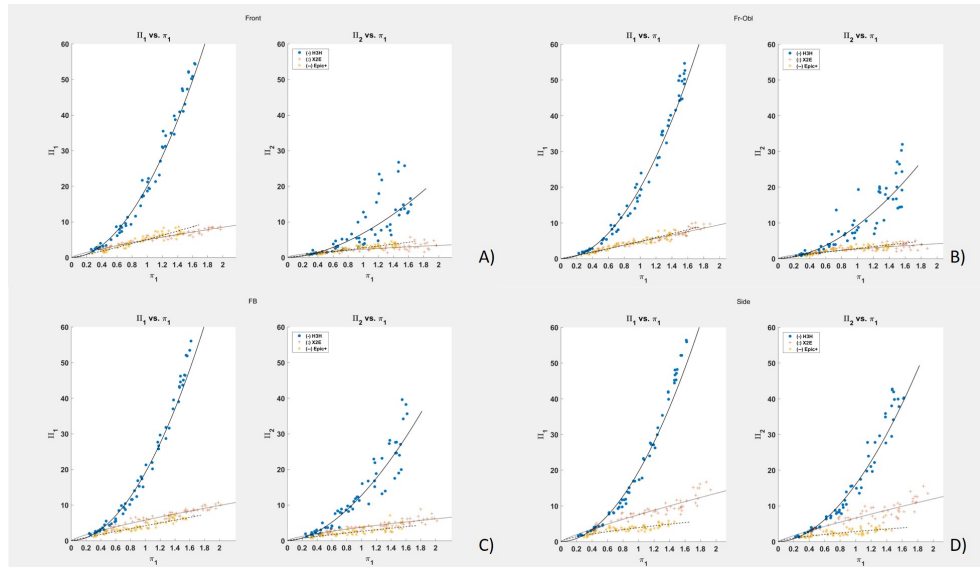


Figure 6.5. Front, Front-Oblique, Front Boss, and Side impact location data appear in A-D respectively for the Xenith helmets tested with this methodology.

The Xenith Epic+ provided a substantial reduction relative to the bare head at 5/8 locations tested with respect to the translational parameter, and 4/8 locations relative to the bare head (Tables 6.8 and 6.9).

Table 6.8.

Effect size measures between each Xenith helmet relative to the bare head for the dimensionless translational acceleration,  $\Pi_1$ . Largest effect size greater than 1 highlighted.

	<b>X2E</b>	<b>Epic+</b>
<b>Forehead</b>	9.91	7.2
<b>F - Oblique</b>	8.28	7.99
<b>Front Boss</b>	8.5	8.62
<b>Side</b>	5.48	6.71
<b>Rear Boss</b>	5.02	7.63
<b>RB - Obl</b>	6.97	7.59
<b>Rear</b>	5.88	5.94
<b>Top</b>	6.28	5

Table 6.9.

Effect size measures between each Xenith helmet relative to the bare head for the dimensionless angular acceleration,  $\Pi_2$ . Largest effect size greater than 1 highlighted.

	<b>X2E</b>	<b>Epic+</b>
<b>Forehead</b>	1.63	1.27
<b>F - Oblique</b>	2.42	2.35
<b>Front Boss</b>	3.66	3.68
<b>Side</b>	3.82	4.83
<b>Rear Boss</b>	1.54	2.84
<b>RB - Oblique</b>	1.23	1.14
<b>Rear</b>	0.33	0.43
<b>Top</b>	1.98	1.27

## 6.5 Discussion

The goal of this study was to quantify the impulse delivered to the headform-helmet system and the resultant translational and angular acceleration to provide a transfer function as previously proscribed by Cummiskey et al. to assess the performance of the newest adult football helmets. An intermediate asymptotic relationship was utilized to provide curve fitting parameters and generate statistical comparisons [37].

Interestingly, the brandwise comparisons revealed that for each brand, relative performance has improved with time for each brand tested despite standards testing from NOCSAE shifting only slightly. This may arise from a number of factors, from mass of the helmets, to the types of padding present. Investigating Riddell helmets, the clear best performing helmet for the translational parameter is the Riddell Speed Flex (Table 6.4). The Riddell Speed Classic performs the best when comparing effect sizes for the dimensionless angular acceleration (Table 6.5) Looking towards Schutt helmets, the Vengeance VTD II had the plurality of largest effect sizes for the translational and angular parameters (Tables 6.6 and 6.7). At the time of the writing of the thesis, the Xenith Epic+ and Xenith X2E perform better at different locations, with the X2E performing best at the front and top, with the Epic+ performing best at the side and rear (Tables 6.8 and 6.9).

Between purely the helmets in 2018 tested relative to one another, some very interesting interplay can be seen (Figures 6.1 and 6.2). The Vicis Zero 1 has some very good performance at the lower end of the impulse parameter, however as the impulse increases, the unique design features in the helmet between the "crumple zone" poles tends to lag behind performance wise, suggesting some tuning between the struts and padding is needed to improve performance of the device. The Xenith Epic+ outperforms the Vicis Zero 1 at some locations and retails for \$350, compared to the \$1500 at the time of writing. It is difficult to say whether the improvements seen at the lower end of impacts delivered to the Hybrid III represent a large enough improvement across the band of impacts seen by players in the field (where the average impact is 37G's or less) to say whether there might be reason to advise purchasing the helmet. The cost differential and metrics in this study make the performance comparison difficult to justify, as the Epic+ has a larger effect size compared to the bare head at more locations for translational acceleration when compared to the Vicis Zero 1.

## 6.6 Acknowledgments

The author would like to thank the Alfred P. Sloan foundation through the Sloan Indigenous Graduate Partnership, the Cordier family, and the Chickasaw Nation Higher Education Foundation who provided support for my work in the form of graduate fellowships and scholarships.

## 7. CONCLUSIONS

All of this work points to one final answer, and that is that helmets are a solvable problem that has not been fully solved yet. Given that the primary modality currently thought to be the source of damage seen in neurotrauma is number and magnitude of HAEs, it is possible to design new helmets by level of play and sport that will significantly alter the amount of acceleration a player will experience on a given impact [13, 14, 19, 40]. The work in Chapter 6 showed that even modern football helmets are a mixed bag when performance comes up, particularly when the price tag on helmets are compared. Currently no better metric exists than the work presented in this study to evaluate quantitatively the effect wearing a helmet has on a head in a lab environment on accelerations experienced at the center of mass of the head. By the metrics presented there, it is difficult to justify the purchase of helmets that retail for \$1500 without knowing the forces that cause accelerations seen by players on field, because in the laboratory, overall performance did not improve substantially over the Xenith Epic+, and while better in front impacts, lagged behind on side and rear impacts. Lacrosse helmets could be improved as well, with better efforts placed in padding the helmets with high quality materials. Soccer headbands need to be redesigned, perhaps with hard outer shells to flex across a surface of padding that can better attenuate energy from impacts.

To design a helmet tailored for a sport and level of play, accurate readings of on-field hits rather than lab recreations are required. This will involve a data collection process with strain gauges and accelerometers placed into the shell of a helmet that passes required certifications for the sport in order to measure in-game and practice hits. After a significant number of hits have been collected, padding can be designed to absorb the most energy along the bandwidth most seen in the sport and level of play (e.g. a Middle School specific Football Helmet, or College specific Hockey

Helmet). This solution also allows for shell design to be tailored as well, as deflection in the shells of a double shell helmet can remove a great deal of energy depending on the compliance of the shell.

Future work should focus on building a basis for thorough, well-designed mathematical simulations of helmeted head impacts. This will be the primary application of CAE in the field of head impact research. In the case of a simple helmet this will require the same techniques applied in aerospace and automotive applications, namely component level models for each type of padding present in a helmet, shell behavior, face mask behavior, and the behavior of any other structure that could affect performance in an impact or crash type environment. After component level material models are validated the assembly level simulations could be validated to a Hybrid III impact model using the same quantitative framework laid out herein. Then once the helmet models have been validated they could be used in combination with player specific head geometries and brain models in order to generate high fidelity models predicting localized damage regions that could be investigated using the same methodologies used by Purdue Neurotrauma Group to track player health, and further improvements to helmets based on the results of those simulations could be generated.

With the growing availability of tools for computer aided engineering and impact simulation becoming more accurate in recent times it is critical that new helmets be analyzed and developed to perform the best in the environment they are going to be used in; this includes tailoring performance as one would a suit for a wedding. After tailoring helmets to level of play, the next step should be the exploration of position specific helmets, as some players within a level of play experience different distributions of hits of different magnitudes. Once the geometries are generated, it is a simple task to swap helmets on a given head model and for a fully-developed helmet + head model, the potential benefits of running parametric sweeps to determine the best helmet design to mitigate the types of hits commonly experienced by a given player are endless. Small changes to helmets already tailored for level of play may not

be the most important factors however, and that difference is well-suited for utilizing sensitivity analyses to determine which parameters have the greatest positive effect on player health.

## REFERENCES

## REFERENCES

- [1] J.E. Bailes, A.L.Petraglia, B.I. Omalu, E.A. Nauman, and T.M. Talavage. Role of subconcussion in repetitive mild traumatic brain injury. *J Neurosurg.*, 119:1235–45, 2013.
- [2] C.W. Hoge, D. McGurk, J.L. Thomas, A.L. Cox, C.C. Engel, and C.A. Castro. Mild traumatic brain injury in u.s. soldiers returning from iraq. *N Engl J Med.*, 358:453–63, 2008.
- [3] J.A. Langlois, W. Rutland-Brown, and M.M. Wald. The epidemiology and impact of traumatic brain injury: a brief overview. *J Head Trauma Rehabil*, 21:375–8, 2006.
- [4] H.L. Laurer, F.M. Bareyre, V.M. Lee, J.Q. Trojanowski, L. Longhi, and R. Hoover et al. Mild head injury increasing the brain’s vulnerability to a second concussive impact. *J Neurosurg.*, 95:859–70, 2001.
- [5] A.C. Mckee, R.C. Cantu, C.J. Nowinski, E.T. Hedley-Whyte, B.E. Gavett, and A.E. Budson et al. Chronic traumatic encephalopathy in athletes: progressive tauopathy after repetitive head injury. *J Neuropathol Exp Neurol.*, 68:709–35, 2009.
- [6] M. Osnato and V. Giliberti. Postconcussion neurosis-traumatic encephalitis a conception of postconcussion phenomena. *Arch NeurPsych*, 18:181–214, 1927.
- [7] H.S. Martland. Punch drunk. *JAMA*, 91:1103–1107, 1928.
- [8] A.G. Gross. A new theory on the dynamics of brain concussion and brain injury. *J Neurosurg*, 15:548–561, 2015.
- [9] A.K. Ommaya, P. Corrao, and F.S. Letcher. Head injury in the chimpanzee part 1: Biodynamics of traumatic unconsciousness. *J Neurosurg.*, 39:152–66, 1973.
- [10] Rates of tbi-related emergency department visits, hospitalizations, and deaths - united states, 2001-2010. CDC.gov, 2016.
- [11] CDC. Traumatic brain injury in the united states. *Available at: <https://www.cdc.gov/traumaticbraininjury/severe.html>*, Accessed 15 January 2019.
- [12] C.M. Baugh, P.T. Kiernan, E. Kroshus, D.H. Daneshvar, P.H. Montenegro, and A.C. McKee et al. Frequency of head-impact-related outcomes by position in ncaa division 1 collegiate football players. *J Neurotrauma.*, 32:98–112, 2015.
- [13] T.M. Talavage, E.A. Nauman, E.L. Breedlove, U. Yoruk, A.E. Dye, and K.E. Morigaki et al. Functionally-detected cognitive impairment in high school football players without clinically-diagnosed concussion. *J Neurotrauma.*, 31:327–38, 2014.

- [14] T.M. Talavage, E.A. Nauman, and L.J. Leverenz. The role of medical imaging in the recharacterization of mild traumatic brain injury using youth sports as a laboratory. *Front Neurol.*, 6:273, 2016.
- [15] B. Johnson, K. Zhang, M. Hallett, and S. Slobounov. Functional neuroimaging of acute oculomotor deficits in concussed athletes. *Brain Imaging Behav*, 9:564–73, 2015.
- [16] K.M. Breedlove, E.L. Breedlove, T.G. Bowman, and E.A. Nauman. Impact attenuation capabilities of football and lacrosse helmets. *J Biomech*, 49:2838–44, 2016.
- [17] V.N. Poole, K. Abbas, T.E. Shenk, E.L. Breedlove, K. M. Breedlove, and M.E. Robinson et al. Mr spectroscopic evidence of brain injury in the non-diagnosed collision sport athlete. *Dev Neuropsychol.*, 39:459–73, 2015.
- [18] V.N. Poole, E.L. Breedlove, T.E. Shenk, K. Abbas, M.E. Robinson, and L.J. Leverenz et al. Sub-concussive hit characteristics predict deviant brain metabolism in football athletes. *Dev Neuropsychol.*, 40:12–17, 2015.
- [19] E.A. Nauman, K.M. Breedlove, E.L. Breedlove, T.M. Talavage, M.E. Robinson, and L.J. Leverenz. Post-season neurophysiological deficits assessed by impact and fmri in athletes competing in american football. *Dev Neuropsychol.*, 40:85–91, 2015.
- [20] K. Abbas, T.E. Shenk, V.N. Poole, E.L. Breedlove, L.J. Leverenz, and E.A. Nauman et al. Alteration of default mode network in high school football athletes due to repetitive subconcussive mild traumatic brain injury: a resting-state functional magnetic resonance imaging study. *Brain Connect*, 40:85–91, 2015.
- [21] D.O. Svaldi, E.C. McCuen, C. Joshi, M.E. Robinson, Y. Nho, and R. Hanne-mann et al. Cerebrovascular reactivity changes in asymptomatic female athletes attributable to high school soccer participation. *Brain Imaging Behav.*, 11:98–112, 2014.
- [22] M.L. Levy, B.M. Ozgur, C. Berry, H.E. Aryan, and M.L. Apuzzo. Birth and evolution of the football helmet. *Neurosurgery*, 55:656–62, 2004.
- [23] J.A. Newman, M.C. Beusenbergh, N. Shewchenko, C. Withnall, and E. Fournier. Verification of biomechanical methods employed in a comprehensive study of mild traumatic brain injury and the effectiveness of american football helmets. *Journal of biomechanics*, 38:1461–81, 2004.
- [24] C. Gadd. Use of a weighted-impulse criterion for estimating injury hazard. *SAE Technical Paper 660793*, 1966.
- [25] F.O. Mueller. Catastrophic head injuries in high school and collegiate sports. *Journal of Athletic Training*, 26:312–15, 2001.
- [26] Standard test method and equipment used in evaluating the performance characteristics of protective headgear/equipment. 2013.
- [27] J. Versace. A review of the severity index. In: *Proceedings of the 15th Stapp Car Crash Conference*, Coronado, CA:771–796, 1971.

- [28] A. Bartsch, E. Benzel, V. Miele, and V. Prakash. Impact test comparisons of 20th and 21st century american football helmets. *J Neurosurg*, 116:222–33, 2012.
- [29] B.I. Omalu, S.T. Dekosky, R.L. Minster, M.I. Kamboh, R.L. Hamilton, and C.H. Wecht. Chronic traumatic encephalopathy in a national football league player. *Neurosurgery*, 57:128–34, 2005.
- [30] R.M. Wright and K.T. Ramesh. An axonal strain injury criterion for traumatic brain injury. *Biomech Model Mechanobiol*, 11:245–260, 2012.
- [31] Standard pneumatic ram test method and equipment used in evaluating the performance characteristics of protective headgear and face guards: Revised July 2018. 2018.
- [32] S. Rowson and S. Dumas. Development of the star evaluation system for football helmets: Integrating player head impact exposure and risk of concussion. *Annals of Biomedical Engineering*, 39:2130–2140, 2011.
- [33] R. Jsdischke, D.C. Viano, N. Dau, A.I. King, and J. McCarthy. On the accuracy of the head impact telemetry (hit) system used in football helmets. *J Biomech*, 46:2310–2315, 2013.
- [34] B. Cummiskey, D. Schiffmiller, T.M. Talavage, L.J. Leverenz, J.J. Meyer, and D. Adams et al. Reliability and accuracy of helmet-mounted and head-mounted devices used to measure head accelerations. *IMEchE Part P: Journal of Sports Engineering and Technology*, 231:144–53, 2017.
- [35] Statement from the national operating committee on standards for athletic equipment regarding 2013 virginia tech star rating system. 2013.
- [36] Standard performance specification for newly manufactured football helmets: Effective May 2019. 2019.
- [37] G.I. Barenblatt. *Scaling, Self-similarity, and Intermediate Asymptotics: Dimensional Analysis and Intermediate Asymptotics*. Cambridge University Press, Cambridge, UK, 1996.
- [38] W. Goldsmith. The state of head injury biomechanics: Past, present and future part 2: Physical experimentation. *Crit Rev Biomed Eng.*, 33:105–207, 2005.
- [39] A.I. King. Fundamentals of impact biomechanics: part i—biomechanics of the head, neck and thorax. *Annu Rev Biomed Eng*, 2:55–81, 2000.
- [40] B. Cummiskey, G.N. Sankaran, K.G. McIver, D. Shyu, J. Markel, T.M. Talavage, L.J. Leverenz, J.J. Meyer, D. Adams, and E.A. Nauman. Quantitative evaluation of impact attenuation by football helmets using a modal impulse hammer. *Journal of Sports Engineering and Technology*, 2019.
- [41] A.J. Padgaonkar, K.W. Krieger, and A.I. King. Measurement of angular acceleration of a rigid body using linear accelerometers. *J Appl Mech*, 42:552–56, 1975.
- [42] S.W. Marshall, K.M. Guskiewicz, V. Shankar, M. McCrea, and R.C. Cantu. Epidemiology of sports-related concussion in seven us high school and collegiate sports. *Inj. Epidemiol.*, 2:13, 2015.

- [43] L.M. Gessel, S.K. Fields, C.L. Collins, R.W. Dick, and R.D. Comstock. Concussions among united states high school and collegiate athletes. *Journal of Athletic Training*, 42:495–503, 2007.
- [44] E. McCuen, D. Svaldi, K. Breedlove, N. Kraz, B. Cummiskey, E.L. Breedlove, and E.A. Nauman. Collegiate women’s soccer players suffer greater cumulative head impacts than their high school counterparts. *J Biomech*, 48:3720–3723, 2015.
- [45] C. Withnall, N. Shewchenko, M. Wonnacott, and J. Dvorak. Effectiveness of headgear in football. *Br J Sports Med*, 39:i40–i48, 2005.
- [46] R.Y. Hinton, A.E. Lincoln, J.L. Almquist, W.A. Douoguih, and K.M. Sharma. Epidemiology of lacrosse injuries in high school-aged girls and boys. *Am J Sports Medicine*, 33:1305–1314, 2005.
- [47] L.R. Vollavanh, K.M. O’Day, E.M. Koehling, and J.M. May et al. Effect of impact mechanism on head accelerations in mens lacrosse athletes. *J Applied Biomechanics*, 34:396–402, 2018.
- [48] K.M. O’Day, E. M Koehling, L.R. Vollavanh, D. Bradney, and J.M. May et al. Comparison of head impact location during games and practices in division iii men’s lacrosse players. *Clinical Biomechanics*, 43:23–27, 2017.
- [49] T.G. Bowman, K.M. Breedlove, E.L. Breedlove, T.M. Dodge, and E.A. Nauman. Impact attenuation properties of new and used lacrosse helmets. *J Biomechanics*, 48:3782–3787, 2015.
- [50] Standard performance specification for newly manufactured lacrosse helmets with faceguard. 2018.
- [51] G.I. Barenblatt. *ASTM F3137-15, Standard Specification for Headgear Used in Womens Lacrosse (excluding Goalkeepers)*. ASTM International, West Conshohocken, PA, 2015.
- [52] R.W. Daniel, S. Rowson, and S.M. Duma. Head impact exposure in youth football: Middle school ages 12-14 years. *Journal of Biomechanical Engineering*, 136:094501–1 – 094501–6, 2014.
- [53] T.J. Young, R.W. Daniel, S. Rowson, and S.M. Duma. Head impact exposure in youth football: Elementary school ages 7-8 years and the effect of returning players. *Clin J Sport Med*, 24:416–421, 2014.
- [54] D.W. Sproule and S. Rowson. Comparison of impact performance between youth and varsity football helmets. *Proc Inst Mech Eng P J Sport Eng Technol.*, 231:374–380, 2018.

## APPENDICES

## A. EXTRA FIGURES FROM 2018 FOOTBALL STUDY

Table A.1.

Parameter values in for A and  $\beta$  in each cell with results from ANCOVA for the dimensionless translational acceleration parameter,  $\Pi_2$  between types of headgear denoted with letters. The annotations, a, b, c, d, and e indicate significant difference ( $p < 0.05$ ) between the regression parameters of the unhelmeted Hybrid III, the Schutt Air XP Pro VTD II, the Vengeance VTD II, the Vengeance Pro, Xenith X2E+, Xenith Epic+, the Speed Flex, the Speed Icon, the Speed Classic, and the Vicis Zero 1.

Locations										
		Front	F-Obl	Front Boss	Side	Rear Boss	RB - Obl	Rear	Fr2	Fr2-Obl
<b>Hybrid III</b>	$A_1$	5.71 (bcdefg)	8.16 (bcdefg)	10.55 (bcdefg)	15.37 (bcdefg)	10.27 (bcdefg)	6.20 (bcdefg)	3.92 (bcdefg)	7.65 (bcdefg)	17.25 (bcdefg)
	$\beta_1$	1.61 (bcdefg)	1.71 (bcdefg)	1.65 (bcdefg)	1.88 (bcdefg)	1.96 (bcdefg)	1.46 (bcdef)	1.29 (bdg)	1.84 (bcdefg)	1.91 (bcdefg)
<b>Schutt Vengeance VTD II</b>	$A_1$	2.79 (acdeg)	2.88 (acefg)	4.17 (acdefg)	3.15 (acdefg)	3.17 (acdef)	3.23 (adef)	2.62 (acdefg)	2.64 (acdefg)	2.90 (acdefg)
	$\beta_1$	1.05 (aefg)	0.94 (aeg)	0.94 (ag)	0.57 (aefg)	0.98 (adg)	1.12 (ag)	0.98 (acf)	0.92 (aeg)	0.97 (aeg)
<b>Schutt Vengeance Pro</b>	$A_1$	5.19 (abdefg)	4.03 (abdefg)	3.20 (abdefg)	3.08 (abdefg)	4.29 (abdefg)	3.24 (adef)	3.60 (abdefg)	3.85 (abdefg)	3.50 (abdefg)
	$\beta_1$	1.01 (aefg)	0.86 (aeg)	0.80 (aefg)	0.60 (aefg)	0.99 (adg)	1.04 (ag)	1.16 (b)	1.01 (aeg)	0.82 (aefg)
<b>Xenith Epic+</b>	$A_1$	2.66 (abcefg)	2.83 (acefg)	2.61 (abcefg)	2.81 (abcefg)	3.44 (abcef)	3.06 (abcef)	3.43 (abcefg)	2.99 (abcefg)	3.06 (abcef)
	$\beta_1$	1.00 (aeg)	0.92 (aeg)	0.86 (aefg)	0.67 (afg)	0.82 (abcefg)	1.09 (ag)	1.12 (a)	0.94 (aeg)	0.90 (aefg)
<b>Riddell SpeedFlex 2018</b>	$A_1$	3.00 (abcdfg)	3.76 (abcdfg)	3.39 (abcdfg)	2.82 (abefg)	2.75 (abcdfg)	2.56 (abcdfg)	2.08 (abcdfg)	4.12 (abcdfg)	4.70 (abcdfg)
	$\beta_1$	1.31 (abcdf)	1.42 (abcdf)	1.05 (acd)	0.77 (abc)	1.05 (adg)	1.02 (ag)	1.14	1.48 (abcdf)	1.39 (abcdf)
<b>Riddell Speed</b>	$A_1$	2.81 (acdeg)	3.16 (abcdeg)	5.23 (abcdeg)	4.40 (abcdeg)	3.25 (abcde)	2.79 (abcdeg)	2.90 (abcdeg)	3.20 (abcdeg)	3.62 (abcdeg)
	$\beta_1$	0.88 (abceg)	1.00 (aeg)	1.07 (acd)	0.87 (abcd)	0.99 (adg)	1.10 (ag)	1.18 (b)	1.01 (aeg)	1.11 (acd)
<b>Vicis Zero 1</b>	$A_1$	1.70 (abdef)	2.20 (abdef)	2.47 (abdef)	2.94 (abdef)	3.32 (ace)	3.27 (aef)	2.37 (abdef)	2.02 (abdef)	3.15 (abcef)
	$\beta_1$	1.31 (abcdf)	1.21 (abcdf)	1.32 (abdef)	0.94 (abcd)	1.40 (abdef)	1.48 (bcdef)	1.10 (a)	1.35 (abcdf)	1.34 (abcdf)

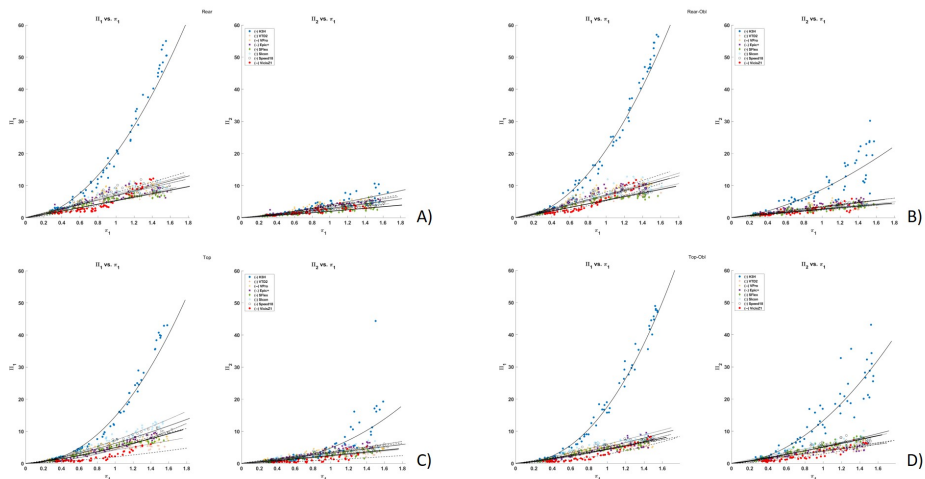


Figure A.1. Rear, Rear-Oblique, Top, and Top-Oblique impact location data appear in A-D respectively for the 2018 football helmets.

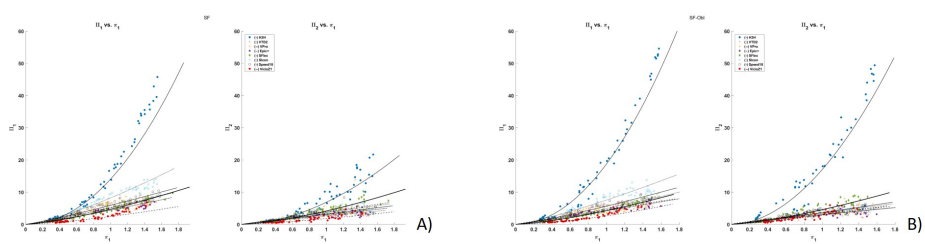


Figure A.2. FR2, and FR2-Oblique impact location data appear in A and B respectively for the 2018 football helmets.

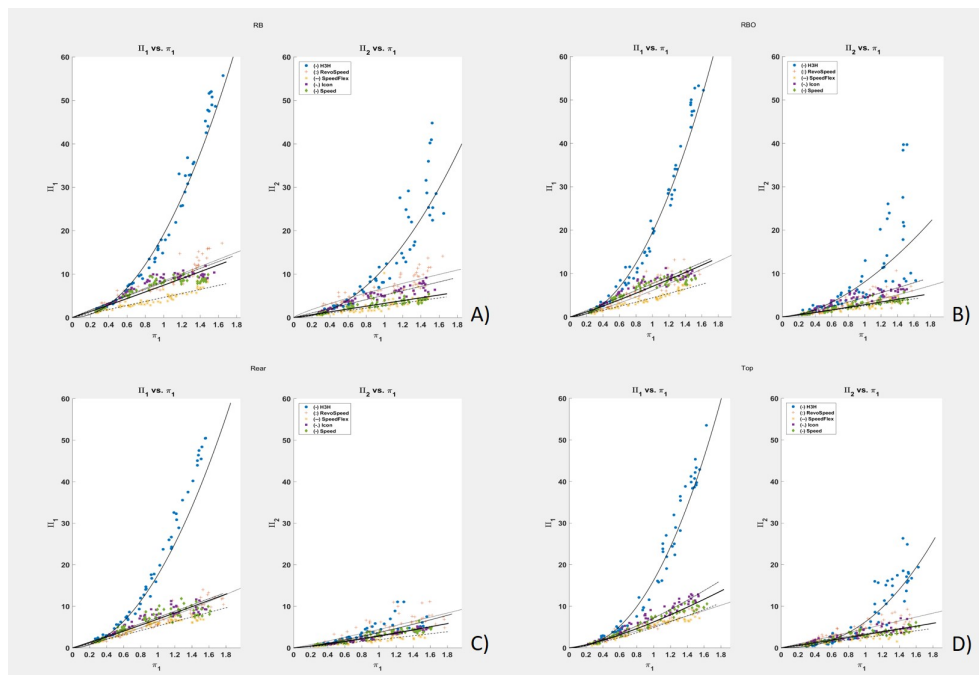


Figure A.3. Rear Boss, Rear Boss Oblique, Rear, and Top impact location data appear in A-D respectively for the Riddell helmets tested with this methodology.

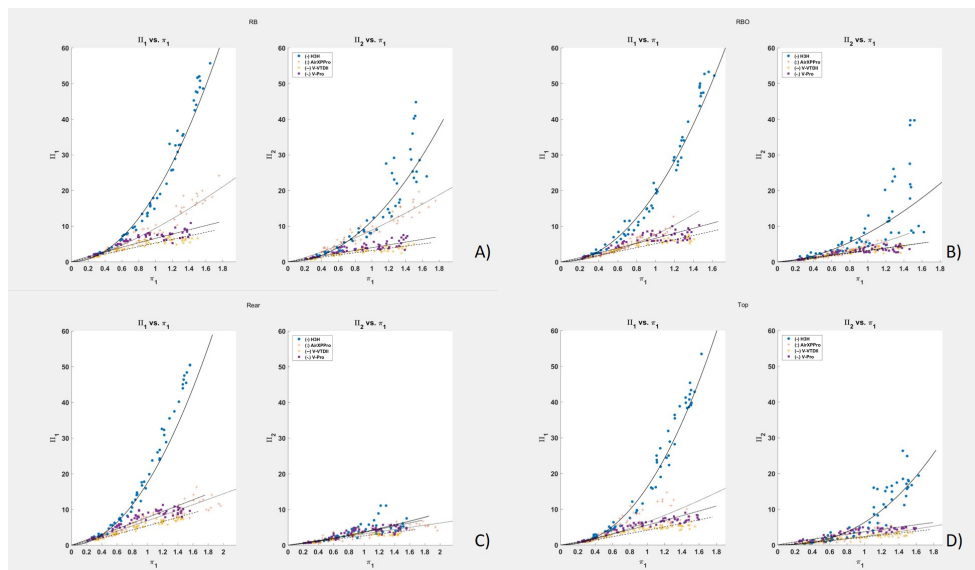


Figure A.4. Rear Boss, Rear Boss Oblique, Rear, and Top impact location data appear in A-D respectively for the Schutt helmets tested with this methodology.

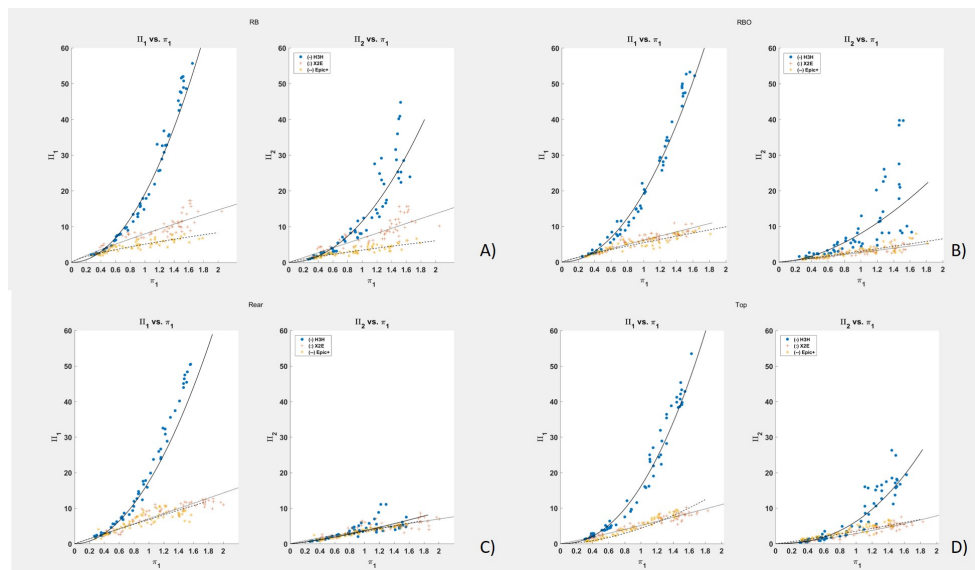


Figure A.5. Rear Boss, Rear Boss Oblique, Rear, and Top impact location data appear in A-D respectively for the Xenith helmets tested with this methodology.